QCD Corrections to $p\bar{p} \to W^+ + X$: A Case Study*

Scott Willenbrock

Physics Department
Brookhkaven National Laboratory
Upton, New York 11973

QCD Corrections to $p\overline{p} \to W^+ + X$:

A Case Study

Scott S. Willenbrock

Physics Department
Brookhaven National Laboratory
Upton, New York 11973

ABSTRACT

We calculate the QCD corrections to inclusive W-boson production in proton-antiproton collisions as an example of a QCD-improved parton model calculation.

1. INTRODUCTION

This year, 1989, marks the twenty-first anniversary of the discovery of what we now know of as quarks inside the proton. The discovery was made at the Stanford Linear Accelerator Center (SLAC) by a SLAC-MIT collaboration, using a 4.5-20 GeV electron beam incident on a liquid hydrogen target.[1] This experiment revealed the existence of point-like constituents of the proton, which were called "partons" by Feynman.[2] Further study at SLAC, as well as at CERN and Fermilab using neutrino beams, led to the conviction that these partons were the quarks which had been proposed in the early sixties by Gell-Mann and Zweig to understand the zoo of hadronic particles.

Another result of these experiments was the realization that quarks alone cannot account entirely for the structure of nucleons. There seemed to be some objects which were invisible to the electron and neutrino beams, but which carried about half the momentum of the proton (in a frame in which the proton is moving relativistically). We now identify these objects as gluons, the quanta of the force which binds the quarks into hadrons. This force is called Quantum Chromodynamics (QCD), and we believe that it is responsible for all of the properties of the strong nuclear force.[3] Today we use the word "parton" to refer collectively to the quarks, antiquarks, and gluons from which we believe all hadrons are constructed.

In the years following the discovery of partons, much theoretical effort was devoted to understanding and justifying the parton model of hadrons. Many of the issues involved were resolved when QCD emerged as the theory of the strong interaction. In particular, QCD provides a framework with which to understand why partons behave as free particles when probed at high momentum transfer, despite the fact that they are permanently confined within hadrons. This phenomenon is a result of the running of the QCD coupling, which decreases with
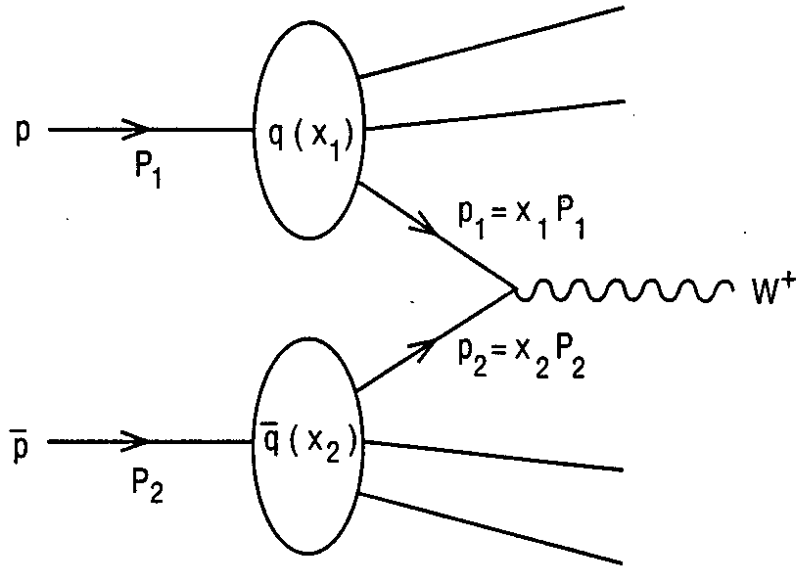
Figure 1: Parton-model picture of inclusive W-boson production in a proton-antiproton collision, $p\bar{p} \to W^+ + X$.

increasing momentum transfer. The static properties of hadrons are governed by low momentum transfer, where the QCD coupling is strong, leading to quark confinement. At high momentum transfer the QCD coupling is sufficiently weak that we may treat the partons as free particles.

Today the emphasis of the parton model has switched from justification to application, although questions of principle still remain. The parton model is an extremely useful tool for performing calculations of high-momentum-transfer processes involving hadrons.[4] In the parton-model picture the proton is regarded as a "bag" of partons, and each parton specie is assigned a distribution function $f(x)$, which is the probability density of finding a parton of specie f carrying a fraction x of the proton's momentum (in a frame in which the proton is moving relativistically). One may then calculate a hadronic cross section by calculating the underlying partonic cross section and convoluting it with the appropriate distribution functions. This is shown diagramatically in Fig. 1 for W-boson production in a proton-antiproton collision. The hadronic cross section for the production of a W boson plus hadrons (denoted by X) is

$$\sigma\left(p\bar{p} \to W^+ + X\right)$$
$$= \sum_{i,j} \int_{\tau_0}^1 dx_1 \int_{\tau_0/x_1}^1 dx_2 \left[q_i\left(x_1\right)\bar{q}_j\left(x_2\right) + \bar{q}_i\left(x_1\right)q_j\left(x_2\right)\right] \hat{\sigma}\left(q\bar{q} \to W^+\right) \quad (1.1)$$

where $\hat{\sigma}$ is the subprocess cross section, $\tau_0 = M_W^2/S$ (where S is the square of the total hadronic center-of-mass energy), and the sum runs over all contributing pairs of partons ($q\bar{q} = u\bar{d}$, $c\bar{s}$, ignoring Cabibbo mixing). The three quarks of which

a proton is made (uud) are called valence quarks. There also exists an ocean of virtual quarks of all flavors, which arises from gluons splitting into $q\overline{q}$ pairs. These are called sea quarks. The parton sum in Eq. (1.1) includes both valence and sea quarks. The second term, in which the proton contributes an antiquark and the antiproton contributes a quark, is entirely due to the presence of sea quarks.

In principle, the parton distribution functions are calculable from QCD. In practice, this is a difficult nonperturbative calculation, since the QCD coupling is strong at an energy scale equal to the proton mass. This difficulty is sidestepped by extracting the distribution functions from the same sort of experiment which was pioneered at SLAC some twenty-one years ago; deep inelastic lepton-nucleon scattering. "Deep" refers to the high-momentum-transfer property of the scattering; "inelastic" means that the target nucleon is destroyed, creating a shower of hadrons; and the lepton beam may consist of electrons (as at SLAC), neutrinos, or muons (the latter two are created as secondary beams at CERN and Fermilab by colliding a proton beam with a nuclear target to produce charged pions, which then decay to muons and muon neutrinos). The nucleon target may consist of any nucleus, with hydrogen and deuterium favored due to their simplicity. Next year a new era of deep inelastic scattering will begin with the commissioning of HERA at DESY, the first machine to collide a lepton beam with a proton beam (30 GeV electrons and 800 GeV protons), rather than with a fixed nuclear target.

The fact that the QCD coupling is weak at high momentum transfer implies that we may perform perturbative calculations of high-momentum-transfer strong-interaction processes. For example, heavy quark production from proton-antiproton collisions may be calculated by convoluting the subprocess cross section for $gg \rightarrow Q\overline{Q}$ with gluon distribution functions:

$$\sigma\left(p\overline{p} \rightarrow Q\overline{Q} + X\right) = \int_{\tau_0}^{1} dx_1 \int_{\tau_0/x_1}^{1} dx_2\, g\left(x_1\right) g\left(x_2\right) \hat{\sigma}\left(gg \rightarrow Q\right) \qquad (1.2)$$

where $\tau_0 = 4m_Q^2/S$. Thus the parton model is useful for calculating strong as well as electroweak processes.

The weakness of the QCD coupling at high momentum transfer also implies that we may reliably calculate QCD radiative corrections to high-momentum-transfer hadronic cross sections. This will be the emphasis of these lectures. QCD radiative corrections to hadronic processes are typically quite large, roughly 30% at momentum transfers of order the W-boson mass. (The corrections are larger at smaller mass scales, due to the increase in the QCD coupling, but eventually become so large that perturbation theory is unreliable.) QCD radiative corrections to electroweak physics thus have the attributes of being large enough to be observed but small enough to be calculated reliably. It is this fortunate situation which makes the study of this topic so rewarding.

The first complete calculation of the QCD radiative corrections to a hadronic process was for the Drell-Yan process, $p\overset{(-)}{p} \rightarrow \mu^+\mu^- + X$, in which the underlying parton reaction is $q\overline{q} \rightarrow \gamma^* \rightarrow \mu^+\mu^-$ (γ^* denotes a virtual photon).[5,6] Today the Drell-Yan process also includes W-boson production, as shown in Fig. 1, as well as
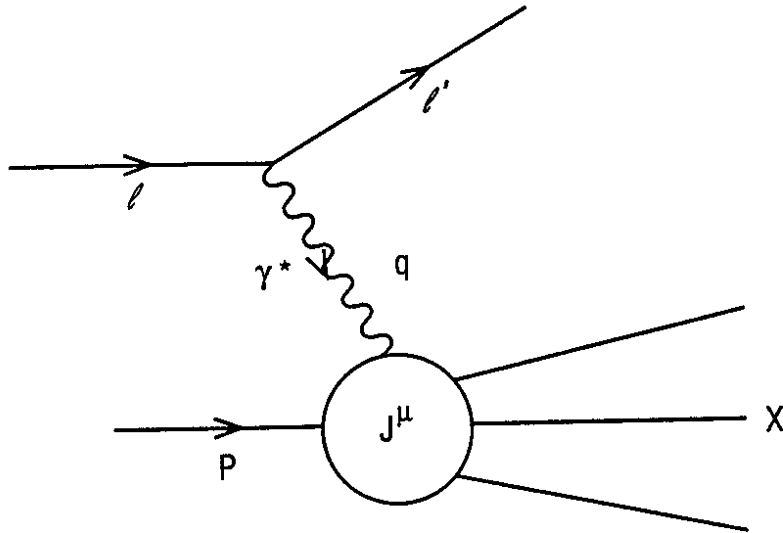
Figure 2: Deep inelastic lepton-proton scattering via a virtual photon.

Z-boson production. These latter two processes were first observed at CERN early in this decade, and are currently undergoing intense study both there and at the Fermilab Tevatron. For concreteness, and because of its current importance, we will concentrate on the calculation of the QCD radiative corrections to W-boson production in $p\bar{p}$ collisions. The concepts and techniques which we encounter along the way are applicable to any parton-model calculation.

Sections 2 and 3 are devoted to deep inelastic scattering. The concepts and notation introduced there are completely standard, and may be found in many textbooks. These sections are important in order to understand how we define the parton distribution functions experimentally.

2. DEEP INELASTIC SCATTERING

Consider the process depicted in Fig. 2, where an incident lepton (electron or muon) of momentum ℓ emits a virtual photon of momentum q and recoils with momentum ℓ', which is measured. The virtual photon strikes a proton of momentum P, dissociating it into a shower of hadrons which we denote X. We define the Lorentz-invariant kinematic variables

$$Q^2 = -q^2 = 2EE'\left(1 - \cos\theta\right) \tag{2.1}$$

$$\nu = \frac{P \cdot q}{M} = E - E' \tag{2.2}$$

where M is the proton mass, E and E' are the lepton energies in the lab frame (the proton rest frame), and θ is the lepton scattering angle in the lab frame.

E' and θ or, equivalently, ν and Q^2, entirely determine the kinematics of the scattering process. Q^2 is the square of the momentum transfer, and the scattering is considered "deep" if $Q^2 >> M^2$.

The amplitude for this deep inelastic scattering process is

$$i\mathcal{M} = (i.e)(-ie)\frac{i}{Q^2}\overline{u}(\ell')\gamma^\mu u(\ell) < P|\, J_\mu\, |X > \qquad (2.3)$$

where e is defined by $\alpha = e^2/4\pi\,(e > 0)$. The lepton spinors are labeled by their momenta, and the spinor product above is referred to as the leptonic current. The quantity $< P|\, J_\mu\, |X >$ is called the hadronic current, and describes the dissociation of the proton. Unlike the leptonic current, it is not possible to calculate the hadronic current perturbatively, since it involves complicated strong-interaction physics. The only thing we know *a priori* about this current is that it is conserved:

$$q^\mu < P|\, J_\mu |X >= 0. \qquad (2.4)$$

This is a consequence of QED, which guarantees that photons couple only to conserved currents.

To obtain the cross section for this process, we first square the amplitude. Summing over final spins and averaging over initial spins, we obtain

$$\overline{|\mathcal{M}|^2} = \frac{1}{2}\frac{1}{2}\sum|\mathcal{M}|^2 = e^4\frac{1}{Q^4}L^{\mu\nu}\frac{1}{2} < P|\, J_\mu|\, X >< X|\, J_\nu|\, P > \qquad (2.5)$$

where (neglecting the lepton mass)

$$L^{\mu\nu} = \frac{1}{2}Tr\slashed{\ell}'\gamma^\mu\slashed{\ell}\gamma^\nu = 2\left(\ell'^\mu\ell^\nu + \ell'^\nu\ell^\mu - g^{\mu\nu}\ell\cdot\ell'\right). \qquad (2.6)$$

The differential cross section is then

$$d\sigma = \frac{1}{2(S - M^2)}\overline{|\mathcal{M}|^2}\frac{d^3\ell'}{(2\pi)^3\,2E'}dX\,(2\pi)^4\,\delta^4\,(P + q - X) \qquad (2.7)$$

where $S = (P + \ell)^2$ and dX denotes the phase space of the final-state hadrons. If we define

$$W_{\mu\nu} = \frac{1}{2}\frac{1}{4\pi M}\int dX < P|\, J_\mu|\, X >< X|\, J_\nu|\, P > (2\pi)^4\,\delta^4\,(P + q - X) \qquad (2.8)$$

then we may write

$$d\sigma = \frac{1}{2(S - M^2)}e^4\frac{1}{Q^4}L^{\mu\nu}4\pi M W_{\mu\nu}\frac{d^3\ell'}{(2\pi)^3\,2E'} \qquad (2.9)$$

where we have integrated out all information about the final hadronic state X. Eq. (2.9) is thus the differential cross section to observe the scattered lepton with momentum ℓ', regardless of the final hadronic state. The process is referred to as

"inclusive," since all final states are included, as opposed to "exclusive," in which a particular hadronic final state is identified.

The only information we have on the hadronic tensor $W_{\mu\nu}$ is based on symmetries. It is Lorentz invariant by construction, and depends only on the momenta P and q, so it must therefore be a linear combination of the five tensors $P_\mu P_\nu$, $P_\mu q_\nu$, $P_\nu q_\mu$, $q_\mu q_\nu$, and $g_{\mu\nu}$ (the tensor $\epsilon^{\mu\nu\rho\sigma} P_\rho q_\sigma$ is eliminated by the parity-conserving nature of QED). Conservation of the hadronic current, Eq. (2.4), tells us that $q^\mu W_\nu = 0$ and $q^\nu W_{\mu\nu} = 0$. These two conditions greatly restrict the structure of $W_{\mu\nu}$ from the five independent tensors listed above to just two. We find

$$
\begin{aligned}
W_{\mu\nu} = &-\left(g_{\mu\nu} - \frac{q_\mu q_\nu}{q^2}\right) W_1\left(\nu, Q^2\right) \\
&+ \frac{1}{M^2}\left(P_\mu - q_\mu \frac{P\cdot q}{q^2}\right)\left(P_\nu - q_\nu \frac{P\cdot q}{q^2}\right) W_2\left(\nu, Q^2\right)
\end{aligned}
\tag{2.10}
$$

where W_1 and W_2 are functions of the kinematic variables ν and Q^2 (the factor M^{-2} is introduced to give W_2 the same dimensions as W_1). These coefficients are referred to as form factors.

The 1968 SLAC-MIT experiment was the first measurement of these form factors at high Q^2 ($Q^2 >> M^2$). The results were startling; the form factor W_1 and the product νW_2, which a priori depend on the two independent variables ν and Q^2, were found to depend only on the ratio Q^2/ν. For this reason it is conventional to define the variable

$$
x \equiv \frac{Q^2}{2M\nu} = \frac{Q^2}{2P\cdot q}
\tag{2.11}
$$

and the form factors

$$
F_1\left(x, Q^2\right) = 2M W_1\left(\nu, Q^2\right)
\tag{2.12}
$$

$$
F_2\left(x, Q^2\right) = \nu W_2\left(\nu, Q^2\right).
\tag{2.13}
$$

The experimental results may then be expressed by stating that F_1 and F_2 are independent of Q^2 at large Q^2. This contrasts sharply with elastic proton form factors (in which the proton remains intact), which decrease like $1/Q^4$ for large Q^2.

The property that F_1 and F_2 are independent of Q^2 at large Q^2 is called Bjorken scaling, and was predicted by Bjorken prior to the SLAC-MIT experiment. It was Feynman who interpreted this scaling property in terms of the parton model, to which we now turn.
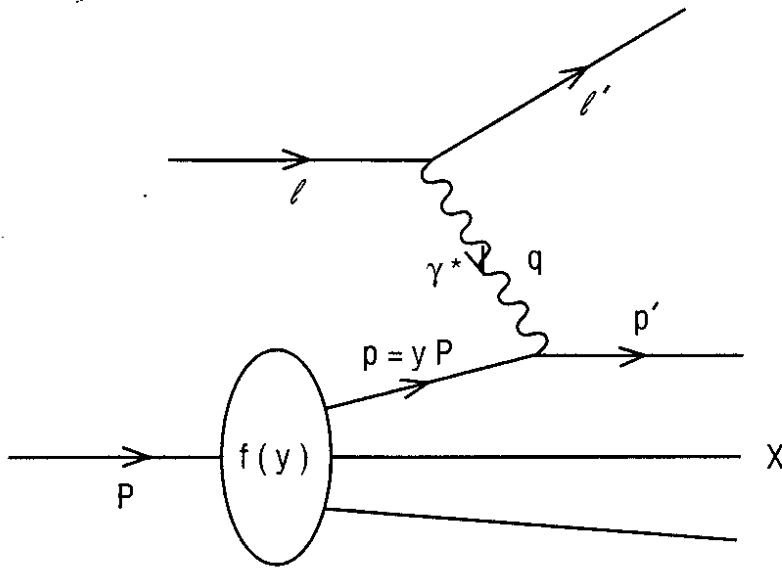
Figure 3: Parton-model picture of deep inelastic lepton-proton scattering.

3. THE PARTON MODEL

The parton-model picture of deep inelastic lepton-nucleon scattering is depicted in Fig. 3. The proton is pictured as a bag of free quarks, antiquarks, and gluons – the three valence quarks are shown in the figure. The virtual photon strikes one of the quarks, which carries a fraction y of the proton's momentum (in a frame in which the proton is moving relativistically), knocking it out of the proton. The final quarks combine into an assortment of hadrons to create the final state X of the preceding section. This "hadronization" is not of any interest to us, since we are summing over all final states.

It is easy to see that the parton model explains Bjorken scaling, i.e., that F_1 and F_2 are independent of Q^2. At zeroth order in QCD, the parton subprocess involved in deep inelastic scattering is simply $\gamma^* q \to q$, as depicted in Fig. 3. Since the quarks are massless, the only energy scale present in this subprocess is Q^2, so the dimensionless form factors F_1 and F_2 cannot depend on Q^2, since there is no other mass with which to form a dimensionless ratio (the parton subprocess does not know about M). However, F_1 and F_2 *can* depend on the dimensionless ratio $x = Q^2/2P \cdot q$. Since the final quark is massless, we find

$$(p+q)^2 = 0 = 2p \cdot q - Q^2. \tag{3.1}$$

Using $p = yP$, this gives

$$x = y. \tag{3.2}$$

Thus, at zeroth order in QCD, the variable x may be identified with the fraction of the proton's momentum carried by the struck parton, and F_1 and F_2 depend only on x.

The parton model allows us to calculate the form factors F_1 and F_2 in terms of the probability density $f(y)$ that the struck quark carries momentum fraction y. Recall from Eq. (2.9) that the hadronic cross section for deep inelastic lepton-nucleon scattering is (for $S >> M^2$)

$$d\sigma = \frac{1}{2S}\frac{e^4}{Q^4}L^{\mu\nu}4\pi M W_{\mu\nu}\frac{d^3\ell'}{(2\pi)^3\,2E'}. \qquad (3.3)$$

The cross section in the parton model is

$$d\sigma = \sum_i \int_x^1 dy\, f_i(y)\, d\hat{\sigma}_i \qquad (3.4)$$

where the sum is over all species of quarks and antiquarks, and $d\hat{\sigma}_i$ is the cross section for the parton subprocess (lepton-quark scattering). We will take Eq. (3.4) as our definition of the quark and antiquark distribution functions at zeroth order in QCD.

The upper limit on the y integral in Eq. (3.4) is obvious; the quark cannot carry more momentum than the proton itself. The lower limit arises in the following way. The scattered quark produces a physical multi-parton state, i.e., a state of positive invariant mass (in Fig. 3, this state is simply one quark). Thus

$$(p+q)^2 \geq 0. \qquad (3.5)$$

Using $p = yP$, this gives

$$2yP \cdot q - Q^2 \geq 0 \qquad (3.6)$$

or

$$y \geq x \qquad (3.7)$$

where $x = Q^2/2P \cdot q$, as defined in the previous section.

The cross section for the lepton-quark scattering subprocess may be written

$$d\hat{\sigma}_i = \frac{1}{2s}\frac{e^4}{Q^4}L^{\mu\nu}\widehat{W}^i_{\mu\nu}\frac{d^3\ell'}{(2\pi)^3\,2E'} \qquad (3.8)$$

where

$$s = (p+\ell)^2 = 2p\cdot\ell = yS \qquad (3.9)$$

and

$$\widehat{W}^i_{\mu\nu} = \frac{1}{2}\int < yP\mid J^i_\mu \mid X' >< X' \mid J^i_\nu \mid yP > dX'\,(2\pi)^4\,\delta^4\left(p+q-X'\right) \qquad (3.10)$$

is the tensor associated with the square of the quark current (the factor 1/2 is from averaging over the initial quark spins). This tensor may be calculated perturbatively, an exercise we will begin shortly. Combining Eqs. (3.4) and (3.8), and comparing the result with Eq. (3.3), we obtain

$$W_{\mu\nu} = \frac{1}{4\pi M}\sum_i \int_x^1 \frac{dy}{y}f_i(y)\,\widehat{W}^i_{\mu\nu} \qquad (3.11)$$

where the factor $1/y$ arises from the lepton-quark flux factor ($s = yS$).

At zeroth order in QCD, the quark current is simply given by the parton subdiagram in Fig. 3. Thus

$$< yP \mid J_\mu^i \mid X' > = < p \mid J_\mu^i \mid p' > = -iq_i \overline{u}(p') \gamma_\mu u(p) \qquad (3.12)$$

where q_i is the quark electric charge (the factor of e associated with the coupling was removed from the current and made explicit in Eq. (2.3)). Thus

$$\widehat{W}_{\mu\nu}^i = \frac{1}{2} q_i^2 \int Tr \not{p}' \gamma_\mu \not{p} \gamma_\nu \frac{d^3 p'}{(2\pi)^3 2E'} (2\pi)^4 \delta^4(p + q - p') . \qquad (3.13)$$

The phase space factor may be written

$$\frac{d^3 p'}{2E'} \delta^4(p + q - p') = d^4 p' \, \delta(p'^2) \, \delta^4(p + q - p')$$
$$= \delta\left((p+q)^2\right) . \qquad (3.14)$$

Performing the trace, we obtain

$$\widehat{W}_{\mu\nu}^i = 2q_i^2 \left(2p_\mu p_\nu + q_\mu p_\nu + q_\nu p_\mu - g_{\mu\nu} p \cdot q\right) 2\pi \, \delta\left(2p \cdot q - Q^2\right) \qquad (3.15)$$

or, using $p = yP$,

$$\widehat{W}_{\mu\nu}^i = 2q_i^2 \left(2y^2 P_\mu P_\nu + y q_\mu P_\nu + y q_\nu P_\mu - y g_{\mu\nu} P \cdot q\right) 2\pi \frac{\delta(y - x)}{2P \cdot q} \qquad (3.16)$$

where we've used $x = Q^2/2P \cdot q$ in the delta function.

We know from Lorentz invariance and current conservation that $W_{\mu\nu}$ has the form given in Eq. (2.10), so $\widehat{W}_{\mu\nu}^i$ must also have this form, since it is related to $W_{\mu\nu}$ via Eq. (3.11). Thus, to isolate the form factors W_1 and W_2, we need only calculate the coefficients of the tensors $P^\mu P^\nu$ and $g^{\mu\nu}$ when we insert Eq. (3.16) into Eq. (3.11). Thus

$$W_{\mu\nu} = \frac{1}{4\pi M} \frac{2\pi}{P \cdot q} \sum_i q_i^2 \int_x^1 \frac{dy}{y} f_i(y) \left(2y^2 P_\mu P_\nu + \cdots - g_{\mu\nu} y P \cdot q\right) \delta(y - x) . \qquad (3.17)$$

Using $\nu = P \cdot q / M$ (see Eq. (2.2)), we obtain

$$W_{\mu\nu} = \sum_i \frac{q_i^2}{M^2 \nu} f_i(x) \left(x P_\mu P_\nu + \cdots - \frac{1}{2} M \nu g_{\mu\nu}\right) . \qquad (3.18)$$

Comparing with our general expression for $W_{\mu\nu}$, Eq. (2.10), we see that

$$W_2 = \sum_i \frac{q_i^2}{\nu} x f_i(x)$$

$$W_1 = \sum_i \frac{q_i^2}{2M} f_i(x) \qquad (3.19)$$

or, using the definitions of F_1 and F_2, Eqs. (2.12) and (2.13),

$$F_1\left(x, Q^2\right) = \sum_i q_i^2 f_i(x) \tag{3.20}$$

$$F_2\left(x, Q^2\right) = \sum_i q_i^2 x f_i(x). \tag{3.21}$$

Thus, at zeroth order in QCD, the form factors F_1 and F_2 are simply related to the sum over the quark and antiquark distribution functions, weighted by the square of the electric charge. As desired, F_1 and F_2 are manifestly independent of Q^2, a consequence of the parton-model picture.

According to Eqs. (3.20) and (3.21), $F_2 = xF_1$, at least at zeroth order in QCD. This equation is known as the Callan-Gross relation. The fact that this relation is upheld experimentally may be construed as evidence that the partons have spin $\frac{1}{2}$, a necessary condition if we are to interpret them as quarks.

The phenomenology of the parton model is a fascinating subject. By using charged lepton (electron and muon), neutrino, and antineutrino beams on hydrogen and deuterium targets, a wealth of information may be gathered, including the shapes of the quark and antiquark distribution functions for each quark flavor, and the separate valence and sea distribution functions for up and down quarks. These topics are beyond the scope of these lectures. They are treated in many excellent textbooks to which the interested reader may turn. None of these topics are necessary for the subject of these lectures, the calculation of QCD corrections to parton-model processes.

4. $p\bar{p} \to W^+ + X$: TREE LEVEL

The first step in our calculation of the QCD corrections to inclusive W-boson production in proton-antiproton collisions is to calculate the lowest-order cross section, as shown in Fig. 1. The partons carry momenta $p_1 = x_1 P_1$ and $p_2 = x_2 P_2$, so the square of the parton center-of-mass energy is

$$s = (p_1 + p_2)^2 = 2p_1 \cdot p_2 = x_1 x_2 S \tag{4.1}$$

where $S = (P_1 + P_2)^2$ is the square of the hadron center-of-mass energy. (Often $\hat{s}$ is used to denote the square of the parton center-of-mass energy and s to denote the square of the hadron center-of-mass energy.) In the case at hand, $s = M_W^2$; in general, however, s is an independent variable. It is conventional to define

$$\tau \equiv s/S = x_1 x_2 \tag{4.2}$$

and to denote the minimum value of τ by τ_0. For example, for the parton subprocess $q\bar{q} \to W^+ g$, the minimum value of s is M_W^2, i.e., there must be at least enough energy to produce a real W boson (the gluon may be arbitrarily energetic, since it is massless), so $\tau_0 = M_W^2/S$. The hadronic cross section is then given in terms

of the partonic cross section and the parton distribution functions by Eq. (1.1). The limits on the x_1 and x_2 integrals are defined by the conditions x_1, $x_2 \leq 1$ and $\tau = x_1 x_2 \geq \tau_0$.

The tree amplitude for the parton subprocess $q\bar{q} \to W^+$ is given by

$$i\mathcal{M} = -i\frac{g}{2\sqrt{2}}\bar{v}(p_2)\gamma^\mu(1-\gamma_5)\,u(p_1)\,\epsilon_\mu(k) \tag{4.3}$$

where the momenta are labeled in Fig. 1 and $\epsilon_\mu(k)$ is the W-boson polarization vector. We now square the amplitude, sum over the W-boson polarization states, and average over the quark spins. We must also average over color; for a given quark color, there is only one chance in three that the antiquark will have the right anticolor to yield a colorless W boson. Thus we obtain

$$\overline{|\mathcal{M}|^2} = \frac{1}{3}\frac{1}{2}\frac{1}{2}\frac{g^2}{8}Tr\not{p}_2\gamma^\mu(1-\gamma_5)\not{p}_1\gamma^\nu(1-\gamma_5)\left(-g_{\mu\nu}+\frac{k_\mu k_\nu}{M_W^2}\right). \tag{4.4}$$

We may discard the $k_\mu k_\nu/M_W^2$ term in the W-boson polarization sum, using

$$\not{p}_2\not{k}(1-\gamma_5)\not{p}_1 = \not{p}_2(\not{p}_1+\not{p}_2)\not{p}_1(1+\gamma_5) = 0 \tag{4.5}$$

since $\not{p}_{1,2}^2 = p_{1,2}^2 = 0$. This is a manifestation of the conservation of the W-boson current,

$$k_\mu\bar{v}(p_2)\gamma^\mu(1-\gamma_5)u(p_1) = \bar{v}(p_2)(\not{p}_1+\not{p}_2)(1-\gamma_5)u(p_1) = 0 \tag{4.6}$$

for massless quarks ($\not{p}_1 u(p_1) = 0$, $\bar{v}(p_2)\not{p}_2 = 0$).

Performing the trace in Eq. (4.4), we obtain

$$\overline{|\mathcal{M}|^2} = \frac{1}{3}\frac{1}{2}\frac{1}{2}\frac{g^2}{8}8s. \tag{4.7}$$

The partonic cross section is given by

$$\hat{\sigma} = \frac{1}{2s}\overline{|\mathcal{M}|^2}\frac{d^3k}{(2\pi)^3\,2E}(2\pi)^4\,\delta^4(p_1+p_2-k). \tag{4.8}$$

Performing a phase-space manipulation similar to Eq. (3.14),

$$\frac{d^3k}{2E}\delta^4(p_1+p_2-k) = d^4k\,\delta(k^2-M_W^2)\,\delta^4(p_1+p_2-k) = \delta(k^2-M_W^2) \tag{4.9}$$

and inserting the expression for $\overline{|\mathcal{M}|^2}$, Eq. (4.7), into Eq. (4.8), we obtain the partonic cross section

$$\hat{\sigma} = \frac{\pi^2}{3}\frac{\alpha}{x_W}\delta(s-M_W^2) \tag{4.10}$$

where $x_W \equiv \sin^2\theta_W$, and $\alpha = e^2/4\pi$, as always.

We now insert the partonic cross section, Eq. (4.10), into Eq. (1.1), to obtain the hadronic cross section. Recalling $s = x_1 x_2 S$, we write

$$\sigma = \frac{\pi^2}{3} \frac{\alpha}{x_W} \sum_{i,j} \int_{\tau_0}^1 dx_1 \int_{\tau_0/x_1}^1 dx_2$$
$$\times \left[q_i(x_1) \overline{q}_j(x_2) + \overline{q}_i(x_1) q_j(x_2) \right] \delta\left(x_1 x_2 S - M_W^2\right). \qquad (4.11)$$

Using the delta function to perform the dx_2 integral, we obtain

$$\sigma = \frac{\pi^2}{3} \frac{\alpha}{x_W} \frac{1}{S} \sum_{i,j} \int_{\tau_0}^1 \frac{dx_1}{x_1} \left[q_i(x_1) \overline{q}_j(\tau_0/x_1) + \overline{q}_i(x_1) q_j(\tau_0/x_1) \right] \qquad (4.12)$$

where $\tau_0 = M_W^2/S$. The sum is over all contributing quark-antiquark combinations ($q\overline{q} = u\overline{d}, \ c\overline{s}$, neglecting Cabbibo mixing).

To complete the calculation, we need to perform the integration over the quark and antiquark distribution functions. The distribution functions are extracted from deep inelastic scattering, as detailed in sections 2 and 3. Several groups have used the available data to construct parameterizations of the parton distribution functions, which can be used to perform the integral in Eq. (4.12) numerically. The most popular sets of parton distribution functions currently available are:

- Glück, Hoffman, and Reya (GHR)[7]

- Duke and Owens (DO)[8]

- Eichten, Hinchliffe, Lane, and Quigg (EHLQ)[9]

- Martin, Roberts, and Stirling (MRS)[10]

- Diemoz, Ferroni, Longo, and Martinelli (DFLM)[11]

- Tung[12]

All of these sets are available as prepackaged computer programs.

To make contact with reality, let's make a rough comparison of our predicted cross section for $p\overline{p} \to W^+ + X$ with the results of the 1988-89 Fermilab Tevatron collider run. Using any of the above listed sets of distribution functions to perform the integral in Eq. (4.12), we find $\sigma\left(p\overline{p} \to W^+ + X\right) \approx 7 \ nb$. Multiplying this by the integrated luminosity of the run, $\int \mathcal{L} dt \approx 5 \ pb^{-1}$, and a factor of 2 to include W^- production, we expect about 7×10^4 W bosons to be produced. The cleanest signal for a W boson in a hadron collider is via its decays to $e\nu_e$ and $\mu\nu_\mu$, each of which has a branching ratio of 1/9 (assuming $W^+ \to t\overline{b}$ is kinematically forbidden, as it appears at this time). Thus we expect about 8,000 $W \to e\nu$ events. Preliminary results on the W-boson production cross section by the CDF collaboration at Fermilab are based on a sample of about 2000 $W \to e\nu$ events. The factor of four discrepancy is due to experimental cuts made on the data and to detector efficiencies.

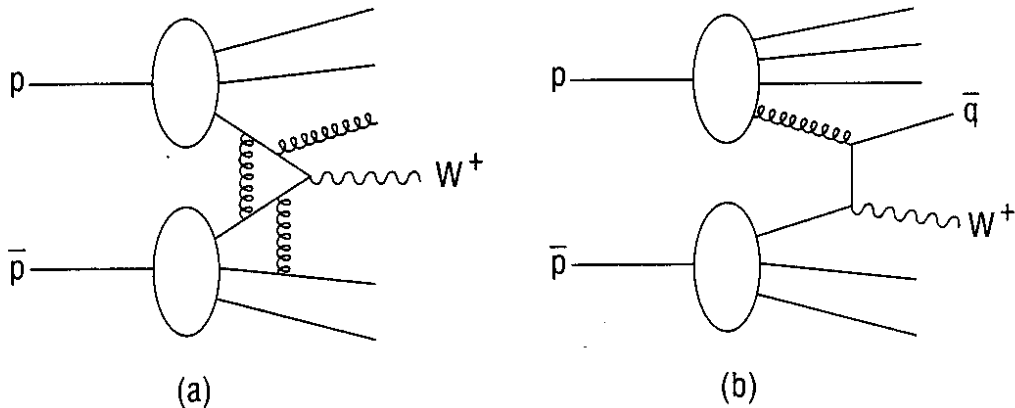**Figure 4:** QCD corrections to $p\bar{p} \to W^+ + X$: (a) virtual gluon, gluon radiation, and gluon exchange between a participant and spectator quark, (b) initial gluon, due to the gluon content of the proton.

5. QCD-IMPROVED PARTON MODEL

We are now prepared to embark on the main subject of these lectures – the calculation of the QCD corrections to W-boson production in $p\bar{p}$ collisions. Some potential corrections are shown in Fig. 4. There are virtual gluon corrections, such as the vertex correction shown in Fig. 4(a). There are corrections due to gluon radiation, also shown in Fig. 4(a). These two processes may be regarded as QCD corrections to the parton subprocess $q\bar{q} \to W^+$.

There are also corrections due to the exchange of a gluon between a parton which participates in the scattering subprocess and a spectator parton, also shown in Fig. 4(a). This type of correction is suppressed by powers of Λ^2/Q^2, where Λ is the QCD scale parameter ($\Lambda \sim 200$ MeV) and Q is the scale of the parton subprocess. Such corrections are referred to as "higher twist," and are totally negligible for the process at hand, in which $Q^2 = M_W^2$. The fact that such corrections are suppressed is important for the validity of the parton model, since they would spoil any attempt to factorize the hadronic cross section into a partonic cross section multiplied by parton distribution functions, as in Eq. (1.1). This factorization has been proven to all orders in QCD perturbation theory for the Drell-Yan process.[13]

There is another class of QCD corrections to W-boson production, shown in Fig. 4(b). These corrections are due to the presence of gluons in the incident hadrons. These diagrams are the same order in the QCD coupling as those of Fig. 4(a), and must therefore be included in a consistent calculation.

There are QCD corrections to the parton distribution functions as well. These must be included along with the corrections to the parton subprocess, since the hadronic cross section is given by a product of distribution functions and the subprocess cross section, as in Eq. (1.1). The distribution functions are defined in terms of deep inelastic scattering, as discussed in sections 2 and 3. Fig. 5
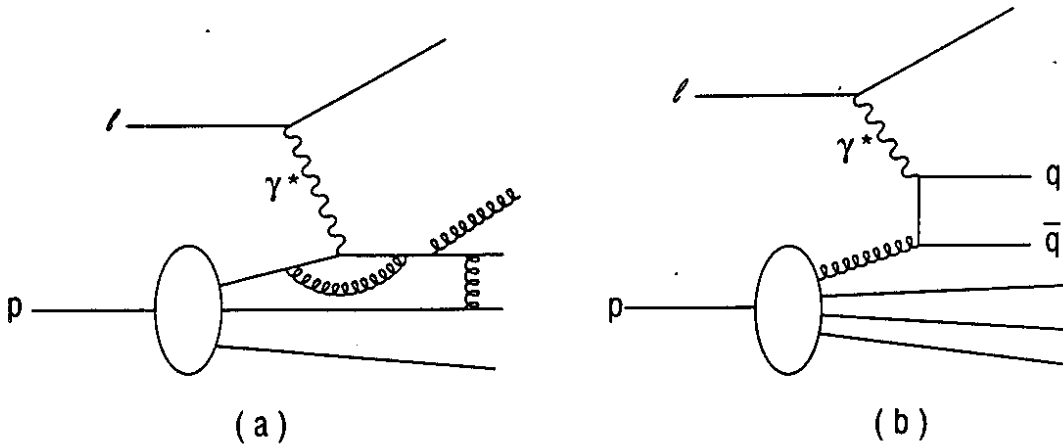
Figure 5: QCD corrections to deep inelastic lepton-proton scattering: (a) virtual gluon, gluon radiation, and gluon exchange between a participant and spectator quark, (b) initial gluon, due to the gluon content of the proton.

shows various QCD corrections to deep inelastic scattering. These corrections are analogous to the corrections to W-boson production in Fig. 4. Fig. 5(a) shows virtual gluon, gluon radiation, and participant-spectator corrections, similar to Fig. 4(a). As before, the correction due to gluon exchange between a participant and spectator parton is higher-twist, i.e., suppressed by powers of Λ^2/Q^2, and may safely be neglected. Fig. 5(b) shows a correction due to the presence of gluons in the hadron target, similar to the correction to W-boson production in Fig. 4(b).

There is another potential roadblock to the factorization of the hadronic cross section into a partonic cross section multiplied by parton distribution functions, as in Eq. (1.1). This is due to the presence of large logarithms encountered in perturbation theory. One finds that the QCD corrections to the parton-model picture are of $\mathcal{O}\left(\alpha_s \ln Q^2/m^2\right)$, where α_s is the QCD coupling, Q is the relevant partonic energy scale, and m is the parton mass ($m << 1$ GeV). Although α_s is small at large Q^2, $\alpha_s \ln Q^2/m^2$ is not, and perturbation theory breaks down. This would spoil the parton-model picture, in which the partons are treated as free particles at zeroth order in QCD.

In order to understand how we handle these large logarithms, we must first understand their source. Consider the first diagram in Fig. 6, in which a W boson is produced in association with a quark. This diagram may be considered as a QCD correction to W-boson production, as in Fig. 4(b). The propagator of the intermediate quark is

$$\frac{i}{\not{p}_3 - \not{p}_1 - m} = i\frac{\not{p}_3 - \not{p}_1 + m}{\left(p_3 - p_1\right)^2 - m^2} = -i\frac{\not{p}_3 - \not{p}_1 + m}{2p_1 \cdot p_3} \tag{5.1}$$

where m is the quark mass $\left(p_3^2 = m^2\right)$. If we choose the gluon to be moving along the z axis, and the final quark to be scattered into the $y - z$ plane by an angle θ,
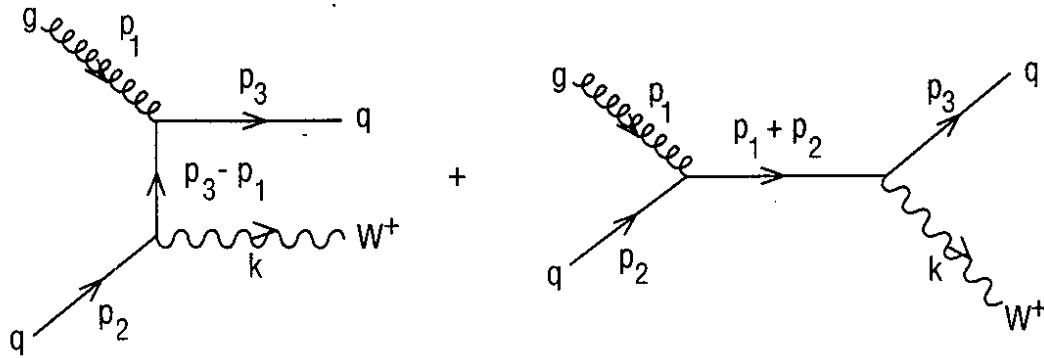
Figure 6: Feynman diagrams for $gq \to W^+ q$.

then we may write the momenta as

$$p_1 = (E_1, 0, 0, E_1)$$
$$p_3 = (E_3, 0, \beta E_3 \sin\theta, \beta E_3 \cos\theta) \quad . \tag{5.2}$$

where β is the velocity of the quark. The denomination of the quark propagator in Eq. (5.1) is thus

$$\frac{1}{2p_1 \cdot p_3} = \frac{1}{2E_1 E_3 \left(1 - \beta\cos\theta\right)}. \tag{5.3}$$

If we set the quark mass to zero, then $\beta = 1$, and we find that the propagator is singular at $\theta = 0$, i.e., at zero scattering angle. This divergence is referred to as a collinear singularity, since the outgoing fermion is moving in the same direction as the incoming gluon. This singularity is avoided if we use a non-zero quark mass, so it is often referred to as a mass singularity. Collinear divergences are also discussed in the lectures by Frank Paige.

To obtain the cross section for the process in Fig. 6, we square the amplitude and integrate over the scattering angle. We find that the square of the first diagram in Fig. 6 gives

$$|\mathcal{M}|^2 \sim \frac{1}{2p_1 \cdot p_3} \tag{5.4}$$

as we will show in section 6. (One would naively expect $|\mathcal{M}|^2 \sim 1/\left(2p_1 \cdot p_3\right)^2$, i.e., the square of the denominator of the quark propagator, but the square of the numerator of the diagram contributes a factor of $2p_1 \cdot p_3$.) Thus, using Eq. (5.3), we find

$$\hat{\sigma} \sim \int_{-1}^{1} dz \, |\mathcal{M}|^2 \sim \int_{-1}^{1} dz \, \frac{1}{1 - \beta z} \tag{5.5}$$

where $z = \cos\theta$. In the limit $\beta \to 1$, the integral diverges logarithmically at the upper limit, corresponding to $\theta = 0$. To make the logarithm explicit, we perform the z integration in Eq. (5.5), and then take the $\beta \to 1$ limit. Using
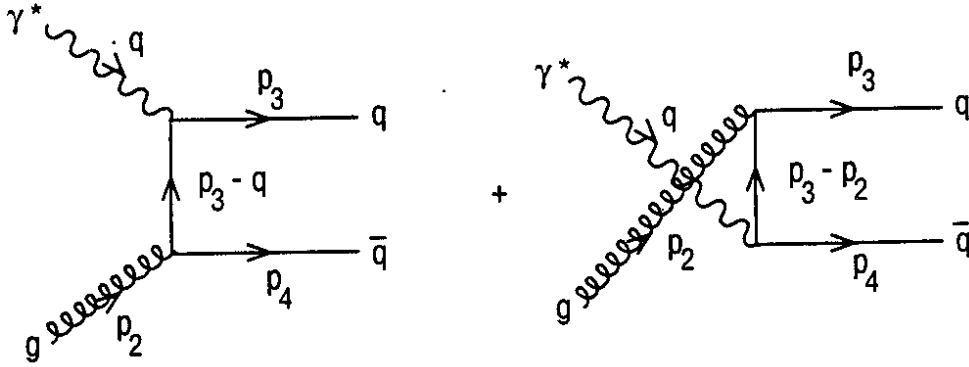
Figure 7: Feynman diagrams for $\gamma^* g \to q\bar{q}$.

$\gamma^2 \equiv 1 - \beta^2 = E_3^2/m^2$, we obtain

$$\hat{\sigma} \sim \frac{1}{\beta} \ln \frac{1+\beta}{1-\beta} \to \ln \frac{4E_3^2}{m^2} \qquad \text{as } \beta \to 1. \tag{5.6}$$

Thus the large logarithm is a result of the collinear divergence in the angular integral. This divergence may be regulated by a non-zero quark mass, as in Eq. (5.6).

The key to eliminating these collinear logarithms is to realize that they occur in both the parton subprocess, as we have just demonstrated, *and* in the corrections to the distribution functions. In deep inelastic scattering, the analogue of the diagram we have just analyzed is the first diagram in Fig. 7. This diagram is singular when the outgoing antiquark is collinear with the incoming gluon, and gives rise to a $\ln Q^2/m^2$. As we said earlier, a complete calculation of the QCD corrections to the hadronic cross section includes the corrections to both the partonic cross section and the distribution functions. As we shall see explicitly, the $\ln m^2$ terms from these two corrections *cancel*, leaving the cross section free of large logarithms, and restoring the validity of perturbation theory. The cancellation of $\ln m^2$ terms has been proven to all orders in QCD perturbation theory.

The cancellation of these logarithms can be understood physically. Consider the first diagram in Fig. 6 which, in the collinear region, looks like Fig. 8(a). The incident gluon splits into a collinear quark and antiquark, and the antiquark annihilates the incident quark to form the W-boson. Now consider the first diagram in Fig. 7 in the collinear region, as depicted in Fig. 8(b). The incident gluon again splits into a collinear quark and antiquark, and the virtual photon finds the quark. In both cases the process factorizes into $g \to q\bar{q}$ times the zeroth-order process ($q\bar{q} \to W^+$ or $\gamma^* q \to q$). The collinear logarithm arises from the $g \to q\bar{q}$ subprocess, and is therefore common to both processes. This is why the collinear logarithms cancel when both corrections are included in the hadronic cross section for W-boson production.

The modern approach to regulating collinear divergences uses dimensional regularization rather than a non-zero quark mass. There are several advantages to the
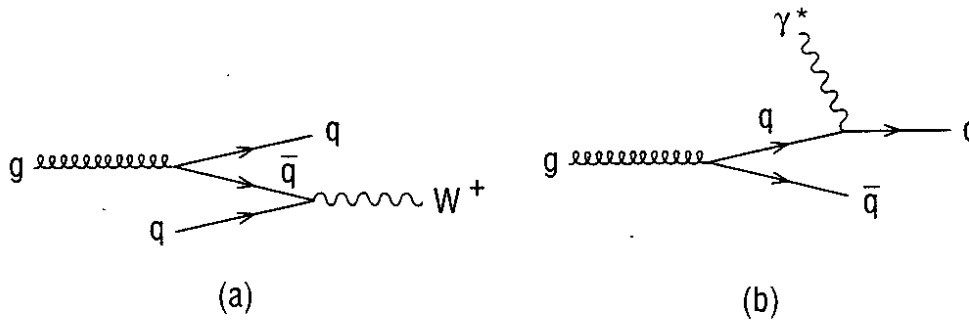
Figure 8: The first diagrams of Figs. 6 and 7 in the collinear region: (a) $gq \to W^+q$, (b) $\gamma^*g \to q\bar{q}$.

use of dimensional regularization. One may use massless kinematics throughout, simplifying the algebra. Other divergences in the calculation, namely infrared and ultraviolet, may also be regulated dimensionally, so the calculation is simplified by using one regulator for all three types of singularities. Finally, it is not known how to extend the quark-mass regulation scheme beyond $\mathcal{O}(\alpha_s)$, while dimensional regularization may be applied to all orders in QCD perturbation theory.

From this point onward these lectures will follow the two original complete calculations of the QCD corrections to the Drell-Yan process, which were published ten years ago. We will mainly follow the discussion of Ref. 5. However, this paper uses a finite quark mass to regulate collinear divergences (and a gluon mass to regulate infrared divergences). Therefore, the calculational details will follow Ref. 6, in which dimensional regularization is used throughout. These papers deal with $pp \to \gamma^* + X$ rather than $p\bar{p} \to W^+ + X$, but the translation is straightforward. Both papers are classics and will reward the reader who studies them carefully.

The remainder of these lectures are organized as follows. We first consider the QCD corrections due to the presence of gluons in the proton, as in Figs. 4(b) and 5(b). We calculate the correction to the partonic cross section in section 6. In section 7 the correction to the quark distribution functions is calculated. The two corrections are combined in sections 8 and 9 to yield the QCD correction to the hadronic cross section from initial gluons. We then tackle the QCD corrections from virtual gluons and gluon radiation. The correction to the partonic cross section, the quark distribution functions, and the hadronic cross section are treated in sections 10, 11, and 12, respectively. We conclude with a discussion of the phenomenology of QCD corrections to W-boson production in $p\bar{p}$ collisions.

6. $gq \to W^+q$

The Feynman diagrams for the process $gq \to W^+q$ are shown in Fig. 6. The amplitude is

$$i\mathcal{M} = -i\frac{g}{2\sqrt{2}}(-ig_s)\,\epsilon^A_\mu(p_1)\,\epsilon_\nu(k)$$

$$\times \bar{u}\left(p_3\right)\left[\gamma^\mu T^A \frac{i}{\not{p}_3-\not{p}_1}\gamma^\nu\left(1-\gamma_5\right)+\gamma^\nu\left(1-\gamma_5\right)\frac{i}{\not{p}_1+\not{p}_2}\gamma^\mu T^A\right]u\left(p_2\right) \quad (6.1)$$

where T^A are the Gell-Mann color matrices and ϵ_μ^A and ϵ_ν are the gluon and W-boson polarization vectors, respectively. Squaring and summing over spins and colors, we obtain

$$|\mathcal{M}|^2 = \frac{g^2}{8}g_s^2 Tr T^A T^A$$

$$\times \left[Tr\not{p}_3\gamma^\mu\left(\not{p}_3-\not{p}_1\right)\gamma^\nu\left(1-\gamma_5\right)\not{p}_2\gamma_\nu\left(1-\gamma_5\right)\left(\not{p}_3-\not{p}_1\right)\gamma_\mu\frac{1}{t^2}\right.$$

$$+ Tr\not{p}_3\gamma^\nu\left(1-\gamma_5\right)\left(\not{p}_1+\not{p}_2\right)\gamma^\mu\not{p}_2\gamma_\mu\left(\not{p}_1+\not{p}_2\right)\gamma_\nu\left(1-\gamma_5\right)\frac{1}{s^2}$$

$$\left.+ 2Tr\not{p}_3\gamma^\mu\left(\not{p}_3-\not{p}_1\right)\gamma^\nu\left(1-\gamma_5\right)\not{p}_2\gamma_\mu\left(\not{p}_1+\not{p}_2\right)\gamma_\nu\left(1-\gamma_5\right)\frac{1}{st}\right] \quad (6.2)$$

where the three terms represent the square of the t-channel diagram, the square of the s-channel diagram, and the cross term, respectively. The $k^\mu k^\nu / M_W^2$ term in the W-boson polarization sum vanishes due to current conservation, as in Eq. (4.5). We have defined the usual Mandelstam variables

$$s = \left(p_1 + p_2\right)^2 = 2p_1 \cdot p_2$$
$$t = \left(p_1 - p_3\right)^2 = -2p_1 \cdot p_3$$
$$u = \left(p_2 - p_3\right)^2 = -2p_2 \cdot p_3 \quad (6.3)$$

for convenience.

To regulate the collinear divergence, we will perform the calculation in $N = 4 - 2\epsilon$ dimensions, and take the limit $\epsilon \to 0$ in the end. The Dirac algebra is defined in any number of dimensions via

$$\{\gamma^\mu, \gamma^\nu\} = 2g^{\mu\nu}. \quad (6.4)$$

We also have

$$g^{\mu\nu}g_{\mu\nu} = N \quad (6.5)$$

since $g_{\mu\nu}$ is the $N \times N$ matrix diag $(1, -1, -1, \cdots, -1)$. Contracting Eq. (6.4) with $g_{\mu\nu}$, we find

$$\gamma^\mu \gamma_\mu = N. \quad (6.6)$$

Using these relations, we may derive the following useful identities:

$$\gamma^\mu \not{a} \gamma_\mu = -2\left(1-\epsilon\right)\not{a} \quad (6.7)$$

$$\gamma^\mu \not{a} \not{b} \gamma_\mu = 4a \cdot b - 2\epsilon\not{a}\not{b} \quad (6.8)$$

$$\gamma^\mu \not{a} \not{b} \not{c} \gamma_\mu = -2\not{c}\not{b}\not{a} + 2\epsilon\not{a}\not{b}\not{c}. \quad (6.9)$$

The Dirac matrices have dimension $2^{N/2}$ for N even, $2^{(N-1)/2}$ for N odd. However, it is consistent to ignore this and to regard them as having dimension four. Thus we will use

$$Tr\,1 = 4 \tag{6.10}$$

where 1 is the unit matrix in Dirac space. There are also ambiguities regarding the definition of γ_5 in N dimensions, but they need not concern us. We will use

$$\{\gamma_\mu,\ \gamma_5\} = 0, \quad \gamma_5^2 = 1 \tag{6.11}$$

as in four dimensions. Also,

$$Tr\,\gamma_5 \slashed{a}\slashed{b} = 0 \tag{6.12}$$

which eliminates traces containing a single γ_5 in all subsequent calculations.

Armed with these relations, we may attack the traces in Eq. (6.2). The first trace gives

$$Tr\slashed{p}_3 \gamma^\mu \left(\slashed{p}_3 - \slashed{p}_1\right) \gamma^\nu \left(1 - \gamma_5\right) \slashed{p}_2 \gamma_\nu \left(1 - \gamma_5\right) \left(\slashed{p}_3 - \slashed{p}_1\right) \gamma_\mu$$
$$= -16 \left(1 - \epsilon\right)^2 st \tag{6.13}$$

where we've used Eq. (6.7) twice, and

$$Tr\slashed{a}\slashed{b}\slashed{c}\slashed{d} = 4 \left[a \cdot b\ c \cdot d + a \cdot d\ b \cdot c - a \cdot c\ b \cdot d\right]. \tag{6.14}$$

The second trace may be obtained from the first via the substitution $p_2 \leftrightarrow -p_3$, or

$$s = (p_1 + p_2) \rightarrow (p_1 - p_3) = t$$
$$t = (p_1 - p_3) \rightarrow (p_1 + p_2) = s, \tag{6.15}$$

i.e., $s \leftrightarrow t$, so the second trace is equal to the first. The third trace, from the cross term, gives

$$Tr\slashed{p}_3 \gamma^\mu \left(\slashed{p}_3 - \slashed{p}_1\right) \gamma^\nu \left(1 - \gamma_5\right) \slashed{p}_2 \gamma_\mu \left(\slashed{p}_1 + \slashed{p}_2\right) \gamma_\nu \left(1 - \gamma_5\right)$$
$$= 16 \left(1 - \epsilon\right) \left(-u M_W^2 + \epsilon st\right) \tag{6.16}$$

where we've used Eq. (6.9), Eq. (6.8), and $Tr\slashed{a}\slashed{b} = 4a \cdot b$, in that order. The relation

$$s + t + u = M_W^2 \tag{6.17}$$

is also useful in the derivation of Eq. (6.16).

Inserting our results for the traces, Eq. (6.2) for the squared amplitude becomes

$$|\mathcal{M}|^2 = 2g^2 g_s^2 Tr T^A T^A \left(1 - \epsilon\right) \left[\left(1 - \epsilon\right) \left(\frac{s}{-t} + \frac{-t}{s}\right) - 2\frac{u M_W^2}{st} + 2\epsilon\right]. \tag{6.18}$$

The collinear region, $p_1 \cdot p_3 \rightarrow 0$, corresponds to $t \rightarrow 0$, so the collinear singularity is apparent in Eq. (6.18). The singularity goes like $1/t$, not $1/t^2$, because the trace in Eq. (6.13) is proportional to t, as mentioned in section 5.

To obtain the cross section, we must average over colors and spins. The incident quark may have one of three colors and the incident gluon one of eight. The Gell-Mann matrices are normalized such that

$$Tr T^A T^B = \frac{1}{2}\delta^{AB} \tag{6.19}$$

so we obtain for the trace in Eq. (6.18)

$$Tr T^A T^A = 4 \tag{6.20}$$

where we've used $\delta^{AB}\delta_{AB} = 8$. Thus the color factor is $\frac{1}{3}\frac{1}{8}4 = \frac{1}{6}$. There are $N-2$ transverse spatial dimensions in N dimensions, so the gluon has $N-2 = 2(1-\epsilon)$ spin components. The quarks have only 2 spin components, since we have chosen to use four-dimensional Dirac matrices (see Eq. (6.10)). Thus the spin- and color-averaged squared amplitude for $gq \rightarrow W^+ q$ is

$$\overline{|\mathcal{M}|^2} = \frac{1}{4}\frac{1}{6}2g^2g_s^2 \left[(1-\epsilon)\left(\frac{s}{-t} + \frac{-t}{s} \right) - 2\frac{uM_W^2}{st} + 2\epsilon \right]. \tag{6.21}$$

The next step in obtaining the cross section is to integrate over the scattering angle of the final particles. N-dimensional phase space gives

$$P.S. = \int \frac{d^{N-1}p_3}{(2\pi)^{N-1}2E_3} \frac{d^{N-1}p_4}{(2\pi)^{N-1}2E_4} (2\pi)^N \delta^N(p_1 + p_2 - p_3 - p_4)$$

$$= \frac{1}{8\pi}\left(\frac{4\pi}{M_W^2} \right)^\epsilon \frac{1}{\Gamma(1-\epsilon)} \left(\frac{M_W^2}{s} \right)^\epsilon \left(1 - \frac{M_W^2}{s} \right)^{1-2\epsilon}$$

$$\times \int_0^1 dv\, v^{-\epsilon}(1-v)^{-\epsilon} \tag{6.22}$$

where v is related to the scattering angle by $v = \frac{1}{2}(1+\cos\theta)$, and $\Gamma(x)$ is the gamma function, defined by

$$\Gamma(x) = \int_0^\infty dt\, e^{-t}t^{x-1}. \tag{6.23}$$

In order to perform the angular integral, we write t and u in terms of v. We find

$$t = -2p_1 \cdot p_3 = -2\frac{\sqrt{s}}{2}\frac{\sqrt{s}}{2}\left(1 - \frac{M_W^2}{s} \right)(1-\cos\theta)$$

$$= -s\left(1 - \frac{M_W^2}{s} \right)(1-v)$$

$$u = -2p_2 \cdot p_3 = -s\left(1 - \frac{M_W^2}{s} \right)v \tag{6.24}$$

where we have used $s + t + u = M_W^2$ to obtain u from t. The cross section for $gq \to W^+ q$ may thus be written

$$
\begin{aligned}
\hat{\sigma} &= \frac{1}{2s} \overline{|\mathcal{M}|^2} P.S. \\
&= \frac{1}{4} \frac{1}{6} \frac{1}{2s} 2g^2 g_s^2 \frac{1}{8\pi} \left(\frac{4\pi}{M_W^2} \right)^\epsilon \frac{1}{\Gamma(1-\epsilon)} \hat{\tau}^\epsilon (1-\hat{\tau})^{1-2\epsilon} \\
&\quad \times \int_0^1 dv\, v^{-\epsilon} (1-v)^{-\epsilon} \left[(1-\epsilon) \left(\frac{1}{(1-\hat{\tau})(1-v)} + (1-\hat{\tau})(1-v) \right) \right. \\
&\quad \left. - 2\hat{\tau} \frac{v}{1-v} + 2\epsilon \right]
\end{aligned}
\tag{6.25}
$$

where we have adopted the notation

$$
\hat{\tau} = \frac{M_W^2}{s}.
\tag{6.26}
$$

The collinear singularity now resides in the v integral; in the limit $\epsilon \to 0$, the v integral is logarithmically divergent at $v = 1$, which corresponds to $\theta = 0$. This divergence is regulated by performing the integral in $N = 4 - 2\epsilon$ dimensions, using

$$
\int_0^1 dv\, v^\alpha (1-v)^\beta = \frac{\Gamma(1+\alpha)\Gamma(1+\beta)}{\Gamma(2+\alpha+\beta)}.
\tag{6.27}
$$

The v integral in Eq. (6.25) yields

$$
\begin{aligned}
(1-\epsilon) &\left(\frac{1}{1-\hat{\tau}} \frac{\Gamma(1-\epsilon)\Gamma(-\epsilon)}{\Gamma(1-2\epsilon)} + (1-\hat{\tau}) \frac{\Gamma(1-\epsilon)\Gamma(2-\epsilon)}{\Gamma(3-2\epsilon)} \right) \\
&- 2\hat{\tau} \frac{\Gamma(2-\epsilon)\Gamma(-\epsilon)}{\Gamma(2-2\epsilon)} + 2\epsilon \frac{\Gamma^2(1-\epsilon)}{\Gamma(2-2\epsilon)}.
\end{aligned}
\tag{6.28}
$$

The collinear singularity now appears as $\Gamma(-\epsilon)$, which diverges as $\epsilon \to 0$.

We may now return to $N = 4$ dimensions by taking the limit $\epsilon \to 0$. We must take this limit carefully, since $\Gamma(-\epsilon) \sim -1/\epsilon$ in this limit. Using

$$
\Gamma(x+1) = x\Gamma(x)
\tag{6.29}
$$

and

$$
\Gamma(n) = (n-1)!, \quad n = \text{integer} \ge 1
\tag{6.30}
$$

we may massage the expression above into the form

$$
-\frac{1}{\epsilon} \frac{\Gamma^2(1-\epsilon)}{\Gamma(1-2\epsilon)} \left(\frac{1-\epsilon}{1-\hat{\tau}} - 2\hat{\tau}(1+\epsilon) \right) + \frac{1}{2}(1-\hat{\tau})
\tag{6.31}
$$

where we've dropped terms of $\mathcal{O}(\epsilon)$ and higher. The collinear singularity now appears as an explicit factor of $1/\epsilon$.

Replacing the v integral in Eq. (6.25) with the expression in Eq. (6.31), we obtain

$$\hat{\sigma} = \frac{1}{4}\frac{1}{6}\frac{1}{2s}2g^2g_s^2\frac{1}{8\pi}\left(\frac{4\pi}{M_W^2}\right)^{\epsilon}\hat{\tau}^{\epsilon}(1-\hat{\tau})^{-2\epsilon}$$
$$\times\left[-\frac{1}{\epsilon}\frac{\Gamma(1-\epsilon)}{\Gamma(1-2\epsilon)}\left[\hat{\tau}^2+(1-\hat{\tau})^2\right]+\frac{3}{2}+\hat{\tau}-\frac{3}{2}\hat{\tau}^2\right] \qquad (6.32)$$

where we've multiplied a factor of $(1-\hat{\tau})$ from phase space into the expression in (6.31). Using

$$-\frac{1}{\epsilon}\left(\frac{4\pi}{M_W^2}\right)^{\epsilon}\hat{\tau}^{\epsilon}(1-\hat{\tau})^{-2\epsilon} = -\frac{1}{\epsilon}\left(1+\epsilon\ln\frac{4\pi}{M_W^2}\frac{\hat{\tau}}{(1-\hat{\tau})^2}+\cdots\right)$$
$$= -\frac{1}{\epsilon}+\ln\frac{M_W^2}{4\pi}\frac{(1-\hat{\tau})^2}{\hat{\tau}} \qquad (6.33)$$

in the limit $\epsilon \to 0$, we obtain our final expression for the spin- and color-averaged cross section for $gq \to W^+q$:

$$\hat{\sigma} = \frac{\pi}{12}\alpha_s\frac{\alpha}{x_W}\frac{1}{s}$$
$$\times\left[\left[\hat{\tau}^2+(1-\hat{\tau})^2\right]\left(-\frac{1}{\epsilon}\frac{\Gamma(1-\epsilon)}{\Gamma(1-2\epsilon)}+\ln\frac{M_W^2}{4\pi}\frac{(1-\hat{\tau})^2}{\hat{\tau}}\right)+\frac{3}{2}+\hat{\tau}-\frac{3}{2}\hat{\tau}^2\right]$$
$$(6.34)$$

where $\alpha_s = g_s^2/4\pi$. Equation (6.34) is also the cross section for $gq \to W^-q$, which is equal to $g\bar{q} \to W^+\bar{q}$ by charge conjugation.

7. $\gamma^*g \to q\bar{q}$

We now consider the correction to the quark distribution functions from the presence of gluons in the proton, as in Fig. 5(b). The Feynman diagrams for the process $\gamma^*g \to q\bar{q}$ are shown in Fig. 7. Our goal is to calculate the contribution of this process to the form factor F_2. We will then use

$$F_2(x,Q^2) \equiv \sum_i q_i^2 x\left[q_i(x,Q^2)+\bar{q}_i(x,Q^2)\right] \qquad (7.1)$$

to *define* the quark distribution functions to all orders in QCD perturbation theory. This is a natural definition of the quark distribution functions because, as we found in Eq. (3.21), $q(x,Q^2) = q(x)$ at zeroth order in QCD.

Alternatively, we could use F_1 to define the quark distribution functions, via Eq. (3.20). This prescription yields a different result for the distribution functions at $\mathcal{O}(\alpha_s)$. Thus the Callan-Gross relation, which at zeroth order is $F_2 = xF_1$, is modified by QCD corrections. It is conventional to use F_2, via Eq. (7.1), to define the distribution functions to all orders in QCD perturbation theory.

In order to extract F_2 from the tensor $W_{\mu\nu}$, it is convenient to define the transverse and longitudinal structure functions

$$W_T \equiv -g^{\mu\nu} W_{\mu\nu} = (3 - 2\epsilon) W_1 - \frac{\nu^2}{Q^2} W_2 \qquad (7.2)$$

$$W_L \equiv P^\mu P^\nu W_{\mu\nu} = -\frac{M^2 \nu^2}{Q^2} W_1 + \frac{M^2 \nu^4}{Q^4} W_2 \qquad (7.3)$$

where we have used the general form for $W_{\mu\nu}$, Eq. (2.10). The calculation is performed in $N = 4 - 2\epsilon$ dimensions, in anticipation of collinear divergences to be encountered. Solving Eqs. (7.2) and (7.3) for W_2, we find

$$(1 - \epsilon) \frac{1}{M} F_2 = x W_T + 4 \frac{x^3}{Q^2} (3 - 2\epsilon) W_L \qquad (7.4)$$

where we've used $F_2 = \nu W_2$ and $x = Q^2 / 2M\nu$, as always.

We now calculate the contribution of the process $\gamma^* g \to q\bar{q}$ to W_T. Contracting Eq. (3.11) with $-g^{\mu\nu}$, we find

$$W_T = \frac{1}{4\pi M} \sum_i \int_x^1 \frac{dy}{y} g(y) \widehat{W_T^i} \qquad (7.5)$$

where $\widehat{W_T^i} = -g^{\mu\nu} \widehat{W_{\mu\nu}^i}$. Recall that $\widehat{W_{\mu\nu}^i}$ is the square of the parton electromagnetic current, integrated over the phase space of the final partons (see Eq. (3.10)). Thus $\widehat{W_{\mu\nu}^i}$ is the square of the amplitude for $\gamma^* g \to q\bar{q}$, with the virtual photon indices contracted with $-g^{\mu\nu}$, integrated over the $q\bar{q}$ phase space.

The calculation of the square of $\gamma^* g \to qq$ is greatly expedited by noticing that it is related, by crossing, to $gq \to W^+ q$, which we calculated in section 6. To go from $gq \to W^+ q$ to $\gamma^* g \to q\bar{q}$, we replace the W boson with the virtual photon, and relabel momenta:

$$p_1 \to p_2$$
$$p_2 \to -p_4$$
$$p_3 \to p_3$$
$$k \to -q. \qquad (7.6)$$

Thus the Mandelstam variables are mapped as follows:

$$s = (p_1 + p_2)^2 \to (p_2 - p_4)^2 = t$$
$$t = (p_1 - p_3)^2 \to (p_2 - p_3)^2 = u$$
$$u = (p_2 - p_3)^2 \to (p_3 + p_4)^2 = s. \qquad (7.7)$$

Recall that the second term in the sum over the W-boson polarizations vanished, leaving simply $-g^{\mu\nu}$, which is what we want for this calculation. We must replace

the weak coupling with the electromagnetic coupling, $g^2 \to 4q_i^2 e^2$. Finally, there is a relative minus sign, since squaring $\gamma^* g \to q\bar{q}$ produces a closed fermion loop, while squaring $gq \to W^+ q$ does not.

Performing these manipulations on the squared amplitude for $gq \to W^+ q$, Eq. (6.18), we obtain

$$ |\mathcal{M}|^2 = -8q_i^2 e^2 g_s^2 Tr T^A T^A (1-\epsilon) \left[-(1-\epsilon) \left(\frac{t}{u} + \frac{u}{t} \right) - 2\frac{sq^2}{tu} + 2\epsilon \right]. \qquad (7.8) $$

Averaging over colors gives the color factor $\frac{1}{8} Tr T^A T^A = \frac{1}{2}$, and averaging over the gluon spin gives a factor $1/2(1-\epsilon)$. Thus the spin- and color-averaged squared amplitude is

$$ \overline{|\mathcal{M}|^2} = \frac{1}{2}\frac{1}{2}8q_i^2 e^2 g_s^2 \left[(1-\epsilon) \left(\frac{t}{u} + \frac{u}{t} \right) - 2\frac{sQ^2}{tu} - 2\epsilon \right]. \qquad (7.9) $$

Collinear divergences are present in the forward ($t \to 0$) and backward ($u \to 0$) regions.

The quark-antiquark phase space is simple, since the quarks are massless. It can be obtained from the W-boson-quark phase space, Eq. (6.22), by setting $M_W = 0$. Thus

$$ P.S. = \int \frac{d^{N-1}p_3}{(2\pi)^{N-1} 2E_3} \frac{d^{N-1}p_4}{(2\pi)^{N-1} 2E_4} (2\pi)^N \delta^N (p_1 + p_2 - p_3 - p_4) $$

$$ = \frac{1}{8\pi} \left(\frac{4\pi}{s} \right)^\epsilon \frac{1}{\Gamma(1-\epsilon)} \int_0^1 dv\, v^{-\epsilon} (1-v)^{-\epsilon} \qquad (7.10) $$

where $v = \frac{1}{2}(1+\cos\theta)$, as usual. Writing t and u in terms of v, we find

$$ t = -2p_2 \cdot p_4 = -2\frac{1}{2}\sqrt{s}\frac{1}{2}\sqrt{s} \left(1 - \frac{q^2}{s} \right) (1 - \cos\theta) $$

$$ = -s \left(1 + \frac{Q^2}{s} \right) (1-v) $$

$$ u = -2p_2 \cdot p_3 = -s \left(1 + \frac{Q^2}{s} \right) v \qquad (7.11) $$

where we have used $s + t + u = -Q^2$ to obtain u from t.

Before performing the angular integral, let us relate s to the usual parton-model variables x and y. The gluon carries fraction y of the proton's momentum, so $p_2 = yP$. Thus

$$ x = \frac{Q^2}{2P \cdot q} = y\frac{Q^2}{2p_2 \cdot q}. \qquad (7.12) $$

Using

$$ s = (p_2 + q)^2 = 2p_2 \cdot q - Q^2 \qquad (7.13) $$

we find

$$s = \frac{y}{x} Q^2 \left(1 - \frac{x}{y} \right) . \tag{7.14}$$

Defining

$$z \equiv \frac{x}{y} \tag{7.15}$$

we obtain

$$s = \frac{Q^2}{z}(1 - z)$$

$$t = -\frac{Q^2}{z}(1 - v)$$

$$u = -\frac{Q^2}{z}v \tag{7.16}$$

where t and u are obtained via Eq. (7.11).

Inserting the expressions for s, t, and u, Eq. (7.16), into the expression for $\overline{\mid \mathcal{M} \mid^2}$, Eq. (7.9), and integrating over the $q\bar{q}$ phase space, Eq. (7.10), we obtain

$$\begin{aligned}
\widehat{W}_T^i &= \overline{\mid \mathcal{M} \mid^2} P.S. \\
&= \frac{1}{2}\frac{1}{2} 8 q_i^2 g_s^2 \frac{1}{8\pi} \left(\frac{4\pi}{Q^2} \frac{z}{1-z} \right)^\epsilon \frac{1}{\Gamma(1-\epsilon)} \\
&\quad \times \int_0^1 dv \, v^{-\epsilon} (1-v)^{-\epsilon} \left[(1-\epsilon) \left(\frac{1-v}{v} + \frac{v}{1-v} \right) - 2z(1-z)\frac{1}{v(1-v)} - 2\epsilon \right] .
\end{aligned} \tag{7.17}$$

(By definition, the factor e^2 is removed, as in Eq. (3.13).) Performing the v integral and taking the limit $\epsilon \to 0$, we obtain

$$\widehat{W}_T^i = 2 q_i^2 \alpha_s \left[z^2 + (1-z)^2 \right] \left(-\frac{1}{\epsilon} \frac{\Gamma(1-\epsilon)}{\Gamma(1-2\epsilon)} + \ln \frac{Q^2}{4\pi} \frac{1-z}{z} \right) \tag{7.18}$$

where the manipulations involved are similar to those used to obtain Eq. (6.31). The collinear divergence once again manifests itself as a factor of $1/\epsilon$. Finally, W_T is obtained by inserting Eq. (7.18) into Eq. (7.5).

Next we calculate the contribution of $\gamma^* g \to q\bar{q}$ to the longitudinal structure function, W_L. Contracting Eq. (3.11) with $P^\mu P^\nu$, we obtain

$$W_L = P^\mu P^\nu W_{\mu\nu} = \frac{1}{4\pi M} \sum_i \int_x^1 \frac{dy}{y^3} f_i(y) \widehat{W}_L^i \tag{7.19}$$

where

$$\widehat{W}_L^i = p_2^\mu p_2^\nu \widehat{W}_{\mu\nu}^i \tag{7.20}$$

and we've used $p_2 = yP$. $\widehat{W}_L^i$ is obtained by contracting the virtual photon index of $\gamma^* g \to q\bar{q}$ with p_2, squaring, and integrating over the $q\bar{q}$ phase space.

Denoting the $\gamma^* g \to q\bar{q}$ amplitude $\mathcal{M}_\mu$, where μ is the photon index, we find

$$p_2^\mu \mathcal{M}_\mu = (-iq_i e)(-ig_s)\bar{u}(p_3)\left[\not{p}_2 \frac{i}{\not{p}_2 - \not{p}_4}\gamma^\nu T^A + \gamma^\nu T^A \frac{i}{\not{p}_3 - \not{p}_2}\not{p}_2\right]v(p_4)\,\epsilon_\nu^A(p_2)$$

$$= (-iq_i e)(-ig_s)\bar{u}(p_3)\left[-2p_4^\nu \not{p}_2 \frac{i}{t} + 2p_3^\nu \not{p}_2 \frac{i}{u}\right]v(p_4)\,\epsilon_\nu^A(p_2) \tag{7.21}$$

where we've used $\not{p}_2^2 = p_2^2 = 0$, and pushed $\not{p}_4$ and $\not{p}_3$ past γ^ν (via Eq. (6.4)) in order to use $\not{p}_4 v(p_4) = \bar{u}(p_3)\not{p}_3 = 0$. Upon squaring and summing over gluon spins $(-g^{\mu\nu})$, the square of each term vanishes, since $p_4^2 = p_3^2 = 0$. Only the cross term survives, yielding

$$p_2^\mu p_2^\nu \mathcal{M}_\mu \mathcal{M}_\nu^* = -q_i^2 e^2 g_s^2 Tr T^A T^A 2(-4p_3 \cdot p_4)\frac{1}{tu}Tr\not{p}_3\not{p}_2\not{p}_4\not{p}_2$$

$$= q_i^2 e^2 g_s^2 Tr T^A T^A 8s. \tag{7.22}$$

The factor $1/tu$ has been cancelled by the numerator, so there are no collinear divergences, and we may calculate in $N = 4$ dimensions henceforth. Averaging over the gluon color $(\frac{1}{8}Tr T^A T^A = \frac{1}{2})$ and spin, we obtain

$$\overline{p_2^\mu p_2^\nu \mathcal{M}_\mu \mathcal{M}_\nu^*} = \frac{1}{2}\frac{1}{2}q_i^2 e^2 g_s^2 8s. \tag{7.23}$$

Since Eq. (7.23) has no angular dependence, the phase space integral, Eq. (7.10), is simply $1/8\pi$. We therefore obtain (removing the factor e^2)

$$\widehat{W_L^i} = q_i^2 \alpha_s Q^2 \frac{1-z}{z} \tag{7.24}$$

where we've used Eq. (7.16) to eliminate s in favor of Q^2 and z. Finally, W_L is obtained by inserting Eq. (7.24) into Eq. (7.19).

Now that we've calculated W_T and W_L, we can insert them into Eq. (7.4) to obtain F_2. Taking the limit $\epsilon \to 0$, we find

$$(1-\epsilon)F_2 = \sum_i q_i^2 \frac{\alpha_s}{2\pi}\int_x^1 dy\, g(y)\, z$$

$$\times \left[\left[z^2 + (1-z)^2\right]\left(-\frac{1}{\epsilon}\frac{\Gamma(1-\epsilon)}{\Gamma(1-2\epsilon)} + \ln\frac{Q^2}{4\pi}\frac{1-z}{z}\right) + 6z(1-z)\right]. \tag{7.25}$$

We now compare this with our definition of the quark distribution functions, Eq. (7.1), to obtain $q(x, Q^2)$ at $\mathcal{O}(\alpha_s)$. Since $\gamma^* g \to q\bar{q}$ contributes equally to the quark and antiquark distribution functions, we obtain

$$q(x, Q^2) = q_0(x)$$

$$+ \frac{\alpha_s}{4\pi}\frac{1}{1-\epsilon}\int_x^1 \frac{dy}{y}g(y)$$

$$\times \left[\left[z^2 + (1-z)^2\right]\left(-\frac{1}{\epsilon}\frac{\Gamma(1-\epsilon)}{\Gamma(1-2\epsilon)} + \ln\frac{Q^2}{4\pi}\frac{1-z}{z}\right) + 6z(1-z)\right]. \tag{7.26}$$

The first term, $q_0(x)$, is the zeroth-order result, and is called the "bare" distribution function. The "renormalized" distribution function, $q(x, Q^2)$, is what one observes experimentally. Since the QCD correction to $q_0(x)$ is infinite (due to the collinear divergence), $q_0(x)$ itself must be infinite in order to yield a finite renormalized distribution function. This conclusion is acceptable, since the bare distribution function is not observable. This situation is analogous to the renormalization of bare coupling constants in field theory.

The quark distribution function, which at zeroth order in QCD is independent of Q^2, becomes dependent on $\ln Q^2$ at $\mathcal{O}(\alpha_s)$. This weak Q^2 dependence has been observed experimentally, and is referred to as a scaling violation. We will return to the topic of the Q^2 dependence of the distribution functions when we discuss the Altarelli-Parisi equations in section 9.

8. $p\overline{p} \to W^+ + X$: INITIAL GLUONS

We can now combine the results of the last two sections to obtain the QCD correction to $p\overline{p} \to W^+ + X$ due to the presence of gluons in the proton. These gluons enter in two ways; as corrections to the subprocess cross section $q\overline{q} \to W^+$, and as corrections to the quark distribution functions. Each of these corrections is collinearly divergent, but these divergences will cancel when combined.

Let's begin by calculating the QCD correction to $p\overline{p} \to W^+ + X$ due to the correction to the quark distribution functions, which was calculated in the previous section. The zeroth-order cross section for $p\overline{p} \to W^+ + X$, Eq. (4.12), was calculated in N = 4 dimensions. Since the QCD correction to the quark distribution functions is collinearly divergent, we must recalculate it in $N = 4 - 2\epsilon$ dimensions. Using Eq. (6.7), we obtain

$$\sigma_0 = \frac{\pi^2}{3} \frac{\alpha}{x_W} (1 - \epsilon) \frac{1}{S} \sum_{i,j} \int_{\tau_0}^1 \frac{dx_1}{x_1} \left[q_{0i}(x_1) \overline{q}_{0j}(\tau_0/x_1) + \overline{q}_{0i}(x_1) q_{0j}(\tau_0/x_1) \right] \quad (8.1)$$

where $\tau_0 = M_W^2/S$. We've placed a subscript on the distribution functions and σ to denote that they are zeroth order in QCD.

The QCD correction to σ_0 due to the correction to the quark distribution functions is obtained by replacing each $\overset{(-)}{q}_0$ in Eq. (8.1) with Eq. (7.26). Let's concentrate on a particular distribution function in Eq. (8.1), say $\overline{q}_{0j}(\tau_0/x_1)$. Eliminating it via Eq. (7.26), we obtain Eq. (8.1) with $\overline{q}_{0j}(\tau_0/x_1)$ replaced by $\overline{q}_j(\tau_0/x_1, Q^2)$, plus the QCD correction term

$$\sigma_1 = -\frac{\pi^2}{3} \frac{\alpha}{x_W} \frac{1}{S} \frac{\alpha_s}{4\pi} \sum_i \int_{\tau_0}^1 \frac{dx_1}{x_1} \int_{\tau_0/x_1}^1 \frac{dx_2}{x_2} q_{0i}(x_1) g(x_2)$$

$$\times \left[\left[z^2 + (1-z)^2 \right] \left(-\frac{1}{\epsilon} \frac{\Gamma(1-\epsilon)}{\Gamma(1-2\epsilon)} + \ln \frac{Q^2}{4\pi} \frac{1-z}{z} \right) + 6z(1-z) \right] \quad (8.2)$$

where
$$z = \frac{\tau_0}{x_1 x_2}. \tag{8.3}$$

Using $s = x_1 x_2 S$, this may be written

$$\sigma_1 = -\frac{\pi}{12}\alpha_s \frac{\alpha}{x_W} \sum_i \int_{\tau_0}^1 dx_1 \int_{\tau_0/x_1}^1 dx_2 \, q_{0i}(x_1) \, g(x_2)$$
$$\times \frac{1}{s}\left[\left[z^2 + (1-z)^2\right]\left(-\frac{1}{\epsilon}\frac{\Gamma(1-\epsilon)}{\Gamma(1-2\epsilon)} + \ln\frac{Q^2}{4\pi}\frac{1-z}{z}\right) + 6z(1-z)\right]. \tag{8.4}$$

We now turn to the QCD correction to the subprocess cross section $q\bar{q} \to W^+$ due to initial gluons. This correction arises via the subprocess $gq \to W^+q$, which was calculated in section 6. Using the usual parton-model formalism, the hadronic cross section due to this subprocess is

$$\sigma_1 = \sum_i \int_{\tau_0}^1 dx_1 \int_{\tau_0/x_1}^1 dx_2$$
$$\times \left[q_{0i}(x_1)\, g(x_2) + \bar{q}_{0i}(x_1)\, g(x_2) + (x_1 \leftrightarrow x_2)\right]\hat{\sigma}\left(gq \to W^+q\right) \tag{8.5}$$

where the proton contributes a parton of momentum fraction x_1 and the antiproton a parton of momentum fraction x_2. Let's concentrate on the first parton combination in Eq. (8.5), $q_{0i}(x_1)\, g(x_2)$. Inserting Eq. (6.34) for $\hat{\sigma}$ into Eq. (8.5), we obtain

$$\sigma_1 = \frac{\pi}{12}\alpha_s \frac{\alpha}{x_W} \sum_i \int_{\tau_0}^1 dx_1 \int_{\tau_0/x_1}^1 dx_2 \, q_{0i}(x_1) \, g(x_2)$$
$$\times \frac{1}{s}\left[\left[\hat{\tau}^2 + (1-\hat{\tau})^2\right]\left(-\frac{1}{\epsilon}\frac{\Gamma(1-\epsilon)}{\Gamma(1-2\epsilon)} + \ln\frac{M_W^2}{4\pi}\frac{(1-\hat{\tau})^2}{\hat{\tau}}\right) + \frac{3}{2} + \hat{\tau} - \frac{3}{2}\hat{\tau}^2\right] \tag{8.6}$$

where $\hat{\tau} = M_W^2/s$. Using $s = x_1 x_2 S$ and $\tau_0 = M_W^2/S$, we find

$$\hat{\tau} = \frac{M_W^2}{s} = \frac{\tau_0}{x_1 x_2} = z, \tag{8.7}$$

i.e., $\hat{\tau}$ in Eq. (8.6) and z in Eq. (8.4) are the same. We shall use $\hat{\tau}$ henceforth in place of z.

We now add the two contributions to σ_1, Eqs. (8.4) and (8.6). The collinear singularities cancel, as anticipated, and we are left with the finite result

$$\sigma_1 = \frac{\pi}{12}\alpha_s \frac{\alpha}{x_W} \sum_i \int_{\tau_0}^1 dx_1 \int_{\tau_0/x_1}^1 dx_2 \, q_{0i}(x_1) \, g(x_2)$$
$$\times \frac{1}{s}\left[\left[\hat{\tau}^2 + (1-\hat{\tau})^2\right]\ln\frac{M_W^2}{Q^2}(1-\hat{\tau}) + \frac{3}{2} - 5\hat{\tau} + \frac{9}{2}\hat{\tau}^2\right] \tag{8.8}$$

where $s = x_1 x_2 S$, $\hat{\tau} = M_W^2/s = \tau_0/x_1 x_2$, and $\tau_0 = M_W^2/S$, as usual.

Equation (8.8) was derived by replacing $\bar{q}_{0j}(\tau_0/x_1)$ in Eq. (8.1) with $\bar{q}_j(\tau_0/x_1, Q^2)$, and by considering only one of four parton combinations in Eq. (8.5). Replacing the other partons in Eq. (8.1) with $q(x, Q^2)$, and considering the other parton combinations in Eq. (8.5), we obtain

$$
\begin{aligned}
\sigma = \frac{\pi^2}{3} \frac{\alpha}{x_W} \frac{1}{S} \sum_{i,j} \int_{\tau_0}^1 dx_1 \int_{\tau_0/x_1}^1 dx_2 \, \delta(x_1 x_2 - \tau_0) \\
\times \left[q_i(x_1, Q^2) \bar{q}_j(x_2, Q^2) + \bar{q}_i(x_1, Q^2) q_j(x_2, Q^2) \right] \\
+ \frac{\pi}{12} \alpha_s \frac{\alpha}{x_W} \sum_i \int_{\tau_0}^1 dx_1 \int_{\tau_0/x_1}^1 dx_2 \left[q_{0i}(x_1) g(x_2) + \bar{q}_{0i}(x_1) g(x_2) + (x_1 \leftrightarrow x_2) \right] \\
\times \frac{1}{s} \left[\left[\hat{\tau}^2 + (1 - \hat{\tau})^2 \right] \ln \frac{M_W^2}{Q^2} (1 - \hat{\tau}) + \frac{3}{2} - 5\hat{\tau} + \frac{9}{2} \hat{\tau}^2 \right].
\end{aligned}
$$

(8.9)

The first term is the zeroth-order cross section, Eq. (8.1), with $q_0(x)$ replaced by $q(x, Q^2)$. The second term represents the $\mathcal{O}(\alpha_s)$ correction to $p\bar{p} \to W^+ + X$ due to the presence of gluons in the proton.

Before evaluating this cross section numerically, we need to discuss the $\ln M_W^2/Q^2$ term in the $\mathcal{O}(\alpha_s)$ term in Eq. (8.9).

9. ALTARELLI-PARISI EQUATION

Equation (8.9) is our result for the $\mathcal{O}(\alpha_s)$ correction to $p\bar{p} \to W^+ + X$ due to the presence of gluons in the proton. The collinear divergences, which appear as terms proportional to $1/\epsilon$ in Eqs. (8.4) and (8.6), have cancelled, leaving a finite result.

In section 5 we argued that collinear divergences lead to factors of $\ln E^2/m^2$, where E is the relevant mass scale and m is a quark mass. Instead of regulating the collinear divergences with a quark mass, we used dimensional regularization. Thus $1/\epsilon$ corresponds to $\ln m^2$, and $\ln E^2$ is the source of the $\ln M_W^2/Q^2$ term in our final result, Eq. (8.9). Thus the $\ln M_W^2/Q^2$ term is associated with the collinear divergences.

The variable Q^2 corresponds to the virtuality of the photon in deep inelastic scattering, which is used to measure the quark distribution functions $q(x, Q^2)$. Typically, $Q^2 \approx (1 - 10 \text{ GeV})^2$, so $\ln M_W^2/Q^2$ is a fairly large factor. Therefore, the terms proportional to $\alpha_s \ln M_W^2/Q^2$ are sufficiently large to invalidate the use of perturbation theory.

Fortunately, there is a way around this problem. The Q^2 dependence of the parton distribution functions is calculable perturbatively, and by evolving $q(x, Q^2)$ to $q(x, M_W^2)$ we can eliminate the $\ln M_W^2/Q^2$ term in Eq. (8.9). The expansion parameter is then simply α_s, and perturbation theory is valid.

To obtain the Q^2 dependence of the quark distribution functions at $\mathcal{O}(\alpha_s)$, we differentiate the QCD-corrected expression for the quark distribution function, Eq. (7.26), with respect to $\ln Q^2$. This gives

$$\frac{d}{d\ln Q^2} q\left(x, Q^2\right) = \frac{\alpha_s}{4\pi} \int_x^1 \frac{dy}{y} g\left(y\right) \left[z^2 + (1-z)^2\right] \tag{9.1}$$

where $z = x/y$. It is conventional to define the "splitting function"

$$P_{qg}\left(z\right) = \frac{1}{2}\left[z^2 + (1-z)^2\right] \tag{9.2}$$

in which case Eq. (9.1) may be written

$$\frac{d}{d\ln Q^2} q\left(x, Q^2\right) = \frac{\alpha_s}{2\pi} \int_x^1 \frac{dy}{y} g\left(y\right) P_{qg}\left(\frac{x}{y}\right). \tag{9.3}$$

The subscript qg on P is to denote that this splitting function refers to quarks coming from gluons splitting, $g \to q\bar{q}$, as in Fig. 8.

Integrating Eq. (9.3) from $\ln Q^2$ to $\ln M_W^2$, we obtain

$$q\left(x, M_W^2\right) = q\left(x, Q^2\right) + \frac{\alpha_s}{4\pi} \ln\frac{M_W^2}{Q^2} \int_x^1 \frac{dy}{y} g\left(y\right) \left[z^2 + (1-z)^2\right]. \tag{9.4}$$

Replacing the $q\left(x, Q^2\right)$ with $q\left(x, M_W^2\right)$ in the zeroth-order cross section for $p\bar{p} \to W^+ + X$ via Eq. (9.4), we find that the $\ln M_W^2/Q^2$ term is eliminated, leaving

$$\sigma = \frac{\pi^2}{3} \frac{\alpha}{x_W} \frac{1}{S} \sum_{i,j} \int_{\tau_0}^1 dx_1 \int_{\tau_0/x_1}^1 dx_2 \, \delta\left(x_1 x_2 - \tau_0\right)$$

$$\times \left[q_i\left(x_1, M_W^2\right) \bar{q}_j\left(x_2, M_W^2\right) + \bar{q}_i\left(x_1, M_W^2\right) q_j\left(x_2, M_W^2\right)\right]$$

$$+ \frac{\pi}{12} \alpha_s \frac{\alpha}{x_W} \sum_i \int_{\tau_0}^1 dx_1 \int_{\tau_0/x_1}^1 dx_2 \left[q_{0i}\left(x_1\right) g\left(x_2\right) + \bar{q}_{0i}\left(x_1\right) g\left(x_2\right) + \left(x_1 \leftrightarrow x_2\right)\right]$$

$$\times \frac{1}{s} \left[\left[\hat{\tau}^2 + (1-\hat{\tau})^2\right] \ln\left(1 - \hat{\tau}\right) + \frac{3}{2} - 5\hat{\tau} + \frac{9}{2}\hat{\tau}^2\right] \tag{9.5}$$

where $s = x_1 x_2 S$, $\hat{\tau} = \tau_0/x_1 x_2$, and $\tau_0 = M_W^2/S$. This is our final result for the $\mathcal{O}(\alpha_s)$ expression for $p\bar{p} \to W^+ + X$ including the effects of initial gluons.

Although we've managed to eliminate the $\ln M_W^2/Q^2$ term from the cross section, it has reappeared in our expression for $q\left(x, M_W^2\right)$, Eq. (9.4). Thus the expansion parameter in Eq. (9.4) is $\alpha_s \ln M_W^2/Q^2$, which again means that perturbation theory is invalid. However, we can sum the leading logarithms, i.e., terms of order $\alpha_s^n \ln^n M_W^2/Q^2$, to all orders in perturbation theory. This is accomplished by replacing the zeroth-order gluon distribution function, $g\left(y\right)$, in the evolution equation, Eq. (9.3), with $g\left(y, Q^2\right)$. Thus the solution to

$$\frac{d}{d\ln Q^2} q\left(x, Q^2\right) = \frac{\alpha_s\left(Q^2\right)}{2\pi} \int_x^1 \frac{dy}{y} g\left(y, Q^2\right) P_{qg}\left(\frac{x}{y}\right) \tag{9.6}$$

incorporates the effects of leading logarithms. Eq. (9.6) is known as an Altarelli-Parisi equation. We have also replaced α_s with $\alpha_s\left(Q^2\right)$ in Eq. (9.6). The running of α_s with Q^2 is also due to summing logarithms, but these logarithms are associated with ultraviolet divergences, and are unrelated to the collinear logarithms which are summed by the Altarelli-Parisi equation. Since we have been calculating at first non-zero order in α_s and $g\left(y\right)$, the Q^2 dependence of these variables has not appeared explicitly. A more thorough treatment of the Altarelli-Parisi equations may be found in the lectures by Frank Paige.

Actually, Eq. (9.6) is only part of an Altarelli-Parisi equation; there is also a term due to quarks emitting gluons, which we will encounter in section 11. There is also an Altarelli-Parisi evolution equation for the gluon distribution function, $g\left(x, Q^2\right)$. Thus, to obtain a complete set of parton distribution functions at $Q^2 = M_W^2$, one begins with input distribution functions at Q^2, taken from experiment, and uses the Altarelli-Parisi equations to evolve them. Since the Altarelli-Parisi equations are coupled integro-differential equations, they must be solved numerically. This is exactly what is done for us in the parton distribution function sets listed at the end of section 4.

We may evaluate the $\mathcal{O}\left(\alpha_s\right)$ correction to $p\overline{p} \rightarrow W^+ + X$ due to initial gluons in Eq. (9.5) by using the aforementioned distribution functions and performing the x_1 and x_2 integrations numerically. We evaluate the quark and gluon distribution functions in the $\mathcal{O}\left(\alpha_s\right)$ correction term at $Q^2 = M_W^2$, just as in the zeroth-order term, to sum leading collinear logarithms. Similarly, we evaluate α_s at $Q^2 = M_W^2$ to sum ultraviolet logarithms.

Evaluating the cross section at the Tevatron energy, $\sqrt{S} = 1.8$ TeV, we find that the $\mathcal{O}\left(\alpha_s\right)$ correction due to initial gluons is only about 7% of the zeroth-order cross section, and is *negative*. At first sight, the sign of the correction is startling; after all, the cross section for $gq \rightarrow W^+q$ is certainly positive. However, the correction to the quark distribution function, Eq. (7.26), makes a negative contribution to the cross section when we replace $q_0\left(x\right)$ with $q\left(x, Q^2\right)$. This negative contribution outweighs the positive contribution from $gq \rightarrow W^+q$.

The correction to $p\overline{p} \rightarrow W^+ + X$ due to the presence of gluons in the proton is thus rather modest. We now turn to the correction due to real and virtual gluon emission, which is numerically more important.

10. $q\overline{q} \rightarrow W^+g$ AND $q\overline{q} \rightarrow W^+$ (ONE LOOP)

We now begin the second half of our calculation of the QCD corrections to $p\overline{p} \rightarrow W^+ + X$; the effect of virtual gluons and gluon radiation. These two types of corrections must be considered together because they are each infrared divergent, but their sum is infrared finite. Virtual gluon and gluon radiation corrections to $q\overline{q} \rightarrow W^+$ are shown in Fig. 4(a); the corresponding corrections to $\gamma^*q \rightarrow q$ are shown in Fig. 5(a). Due to lack of space and time, we will not be able to treat these corrections with the same detail as we treated the corrections due to initial
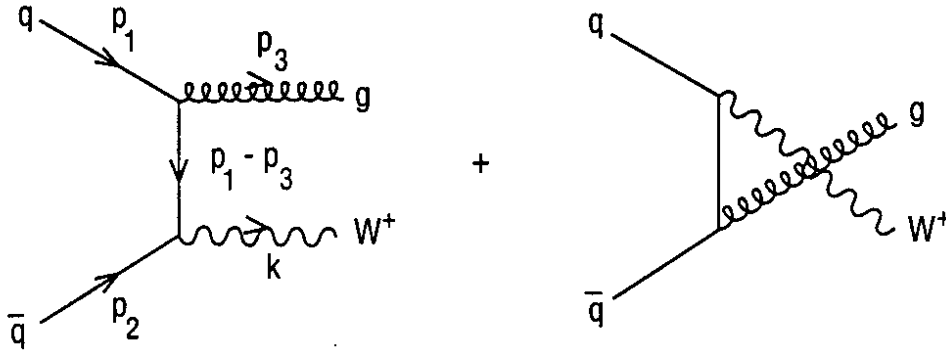
Figure 9: Feynman diagrams for $q\bar{q} \to W^+g$.

gluons in sections 6-9. We will therefore concentrate on the concepts, and leave the calculational details to the interested reader.

Let's begin with a study of the infrared and collinear divergences which we will encounter in this calculation. Consider the first diagram in Fig. 9, which contributes to $q\bar{q} \to W^+g$. The denominator of the quark propagator is

$$\frac{1}{(p_1 - p_3)^2} = \frac{1}{-2E_1 E_3 (1 - \cos\theta)} \tag{10.1}$$

as we showed in section 5. We immediately recognize the familiar collinear singularity as $\theta \to 0$. There is also a singularity when the gluon energy vanishes, $E_3 \to 0$. This is an infrared singularity, and we refer to the gluon as "soft", since it carries little energy. (The reader may object that the same infrared singularity should appear in the process $gq \to W^+q$, which we treated in section 6, because the denominator of the quark propagator in that case is identical to Eq. (10.1). The reason we did not encounter an infrared singularity in that case is that the spinor of the final-state quark, $u(p_3)$, vanishes as $E_3 \to 0$, i.e., as $p_3 \to 0$ (for a massless quark). Thus the potential infrared singularity is cancelled by the quark spinor – there is no divergence associated with a soft quark.)

Consider now the virtual gluon correction to $q\bar{q} \to W^+$, shown in Fig. 10. The loop integral associated with the first diagram is proportional to

$$\int d^4k \, \frac{1}{k^2 (k + p_1)^2 (k - p_2)^2} = \int d^4k \, \frac{1}{k^2 (k^2 + 2k \cdot p_1)(k^2 - 2k \cdot p_2)}. \tag{10.2}$$

If the virtual gluon is soft, i.e., $k \to 0$, the integrand may be approximated by

$$\frac{-1}{k^2 \, 2k \cdot p_1 \, 2k \cdot p_2}. \tag{10.3}$$

Since there are four powers of k in the denominator, the d^4k integral is logarithmically divergent as $k \to 0$. This infrared divergence cancels the infrared divergence
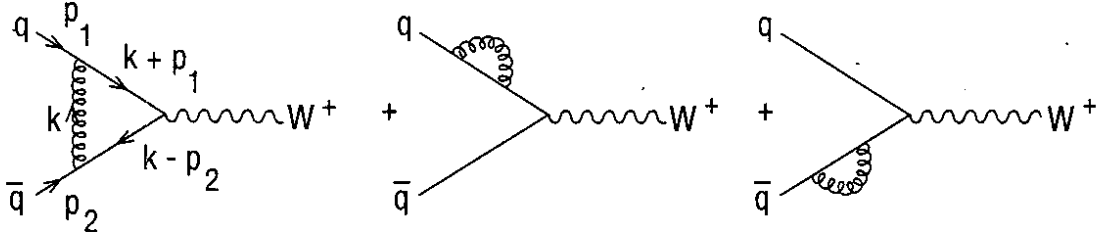
Figure 10: Feynman diagrams for the one-loop corrections to $q\bar{q} \to W^+$.

due to the emission of a real, soft gluon. Infrared divergences are also discussed in the lectures by Frank Paige.

There is also a collinear divergence associated with this loop integral. If $k \sim p_1$, which implies $k^2 \to 0$, then the integrand of Eq. (10.2) is approximately proportional to

$$\frac{-1}{k^2 \, k^2 \, 2p_1 \cdot p_2}.$$ (10.4)

The integrand is again logarithmically divergent. There is also a collinear divergence for $k \sim p_2$. These collinear divergences do not cancel with those from real, collinear gluon emission. Rather, they are all cancelled by similar collinear divergences present in the QCD corrections to the quark distribution functions, exactly as we saw for initial gluons in section 8.

The loop integrals associated with the loop diagrams in Fig. 10 are also ultraviolet divergent. However, the sum of the diagrams is ultraviolet finite, due to a Ward identity which relates the ultraviolet divergences. Thus we need only deal with infrared and collinear divergences. As before, these will be handled by using dimensional regularization.

The correction to the $q\bar{q} \to W^+$ vertex due to virtual gluons, shown in Fig. 10, is

$$i\Gamma^\mu = -i\frac{g}{2\sqrt{2}}\gamma^\mu\left(1 - \gamma_5\right)$$

$$\times \left[1 + \frac{\alpha_s}{4\pi}\frac{4}{3}\left(\frac{4\pi}{-M_W^2}\right)^\epsilon \frac{\Gamma\left(1 + \epsilon\right)\Gamma^2\left(1 - \epsilon\right)}{\Gamma\left(1 - 2\epsilon\right)}\left(-\frac{2}{\epsilon^2} - \frac{3}{\epsilon} - 8\right)\right]$$ (10.5)

where the first term in brackets is the zeroth-order vertex. The $1/\epsilon$ term in the QCD correction is due to the collinear divergence. The $1/\epsilon^2$ term is due to the product of an overlapping collinear and infrared divergence. The overlap occurs because the infrared limit, $k \to 0$, is a special case of the collinear limit, $k \sim p_1$ (or $k \sim p_2$). The factor of 4/3 is a color factor, $T^A T^A = \frac{4}{3}\mathbf{1}$, where $\mathbf{1}$ is a 3×3 unit matrix in color space.

Notice that the QCD correction to the $q\bar{q} \to W^+$ vertex in Eq. (10.5) contains a factor $(-1)^\epsilon$. Expanding this factor in powers of ϵ, we find

$$Re\,(-1)^\epsilon = 1 - \frac{1}{2}\epsilon^2\pi^2$$ (10.6)

where we've used the identity

$$z^\epsilon = e^{\epsilon \ln z} = 1 + \epsilon \ln z + \frac{1}{2}\epsilon^2 \ln^2 z + \cdots \qquad (10.7)$$

for $z = -1$. The reason we take the real part in Eq. (10.6) is that when we square Eq. (10.5) to obtain the cross section, the $\mathcal{O}(\alpha_s)$ correction will come from the interference of the loop correction and the zeroth-order term. Since the latter is real, only the real part of the loop correction will survive.

Replacing the $(-1)^\epsilon$ factor in Eq.(10.5) with the expansion in Eq. (10.6) generates a term proportional to π^2. The expansion

$$\Gamma(1 + \epsilon)\,\Gamma(1 - \epsilon) = 1 + \frac{\pi^2}{6}\epsilon^2 + \cdots \qquad (10.8)$$

also generates a π^2 term. We therefore obtain

$$i\Gamma^\mu = -i\frac{g}{2\sqrt{2}}\gamma^\mu (1 - \gamma_5)$$
$$\times \left[1 + \frac{\alpha_s}{4\pi}\frac{4}{3}\left(\frac{4\pi}{M_W^2}\right)^\epsilon \frac{\Gamma(1-\epsilon)}{\Gamma(1-2\epsilon)}\left(-\frac{2}{\epsilon^2} - \frac{3}{\epsilon} - 8 + \frac{2}{3}\pi^2\right)\right]. \qquad (10.9)$$

Using this QCD-corrected vertex to calculate the spin- and color-averaged cross section, as in section 4, we obtain

$$\hat{\sigma} = \frac{\pi^2}{3}\frac{\alpha}{x_W}\delta\left(s - M_W^2\right)$$
$$\times \left[1 + \frac{\alpha_s}{2\pi}\frac{4}{3}\left(\frac{4\pi}{M_W^2}\right)^\epsilon \frac{\Gamma(1-\epsilon)}{\Gamma(1-2\epsilon)}\left(-\frac{2}{\epsilon^2} - \frac{3}{\epsilon} - 8 + \frac{2}{3}\pi^2\right)\right] \qquad (10.10)$$

where the first term in brackets is the zeroth-order cross section and the second term is the $\mathcal{O}(\alpha_s)$ QCD correction.

The QCD correction to $q\bar{q} \to W^+$ due to real gluon emission is shown in Fig. 9. The squared amplitude for this process can be obtained from that of $gq \to W^+q$, Eq. (6.18), via the replacements $s \to t$, $t \to u$, and $u \to s$, and multiplying by an overall minus sign. The cross section is

$$\hat{\sigma} = \frac{\pi^2}{3}\frac{\alpha}{x_W}\frac{\alpha_s}{2\pi}\frac{4}{3}\left(\frac{4\pi}{M_W^2}\right)^\epsilon \frac{\Gamma(1-\epsilon)}{\Gamma(1-2\epsilon)}\frac{1}{s}$$
$$\times \left[\frac{2}{\epsilon^2}\delta(1-\hat{\tau}) - \frac{2}{\epsilon}\frac{1+\hat{\tau}^2}{(1-\hat{\tau})_+} + 4(1+\hat{\tau}^2)\left(\frac{\ln(1-\hat{\tau})}{1-\hat{\tau}}\right)_+ - 2\frac{1+\hat{\tau}^2}{1-\hat{\tau}}\ln\hat{\tau}\right] \qquad (10.11)$$

where $\hat{\tau} = M_W^2/s$, as always. The relation

$$\hat{\tau}^\epsilon(1-\hat{\tau})^{-1-\epsilon} = -\frac{1}{\epsilon}\delta(1-\hat{\tau}) + \frac{1}{(1-\hat{\tau})_+} - \epsilon\left(\frac{\ln(1-\hat{\tau})}{1-\hat{\tau}}\right)_+$$
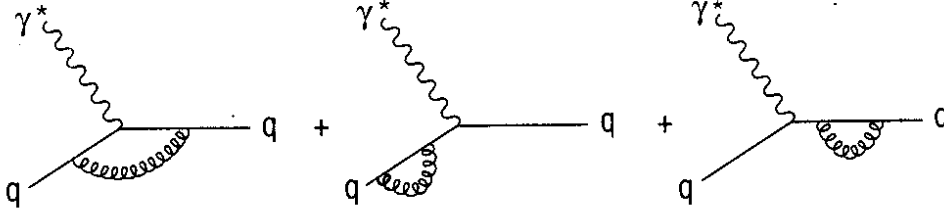$$+ \epsilon\frac{\ln\hat{\tau}}{1-\hat{\tau}} + \mathcal{O}(\epsilon^2) \qquad (10.12)$$

Figure 11: Feynman diagrams for the one-loop corrections to $\gamma^* q \to q$.

was used to derive Eq. (10.11), where the "plus prescription" is defined by

$$\int_0^1 dz \left(g(z) \right)_+ h(z) = \int_0^1 dz \, g(z) \left[h(z) - h(1) \right]. \qquad (10.13)$$

The $(\ )_+$ terms are therefore finite at $\hat{\tau} = 1$, i.e., $s = M_W^2$, which corresponds to the soft-gluon limit. The infrared divergence is contained in the $1/\epsilon^2$ term, which is the product of an overlapping infrared and collinear divergence. This overlap occurs because the infrared limit, $p_3 \to 0$, is a special case of the collinear limit, $p_3 \sim p_1$. The $1/\epsilon$ term in Eq. (10.11) corresponds to a pure collinear divergence.

Adding the virtual and real gluon corrections, Eq. (10.10) and Eq. (10.11), we obtain the QCD-corrected cross section for $q\bar{q} \to W^+$,

$$
\begin{aligned}
\hat{\sigma} =\ & \frac{\pi^2}{3} \frac{\alpha}{x_W} \frac{1}{s} \delta(1 - \hat{\tau}) \\
& + \frac{2\pi}{9} \alpha_s \frac{\alpha}{x_W} \frac{1}{s} \left[\left(\frac{1 + \hat{\tau}^2}{(1 - \hat{\tau})_+} + \frac{3}{2} \delta(1 - \hat{\tau}) \right) \left(-\frac{2}{\epsilon} \frac{\Gamma(1 - \epsilon)}{\Gamma(1 - 2\epsilon)} + 2 \ln \frac{M_W^2}{4\pi} \right) \right. \\
& \left. + 4 \left(1 + \hat{\tau}^2 \right) \left(\frac{\ln(1 - \hat{\tau})}{1 - \hat{\tau}} \right)_+ - 2 \frac{1 + \hat{\tau}^2}{1 - \hat{\tau}} \ln \hat{\tau} + \left(\frac{2}{3} \pi^2 - 8 \right) \delta(1 - \hat{\tau}) \right] \quad (10.14)
\end{aligned}
$$

where $\hat{\tau} = M_W^2/s$. The infrared divergences, proportional to $1/\epsilon^2$, have cancelled, leaving the collinear divergence, proportional to $1/\epsilon$. This divergence will cancel with the collinear divergence present in the QCD correction to the quark distribution functions, a topic to which we now turn.

11. $\gamma^* q \to gq$ AND $\gamma^* Q \to Q$ (ONE LOOP)

We now consider the QCD corrections to the quark distribution functions due to virtual and real gluon emission. As before, the quark distribution functions are defined in terms of the form factor F_2, measured in deep inelastic scattering, via Eq. (7.1).

The virtual-gluon corrections to deep inelastic scattering are shown in Fig. 11. The diagrams are identical to those of $q\bar{q} \to W^+$, Fig. 10, with the W boson

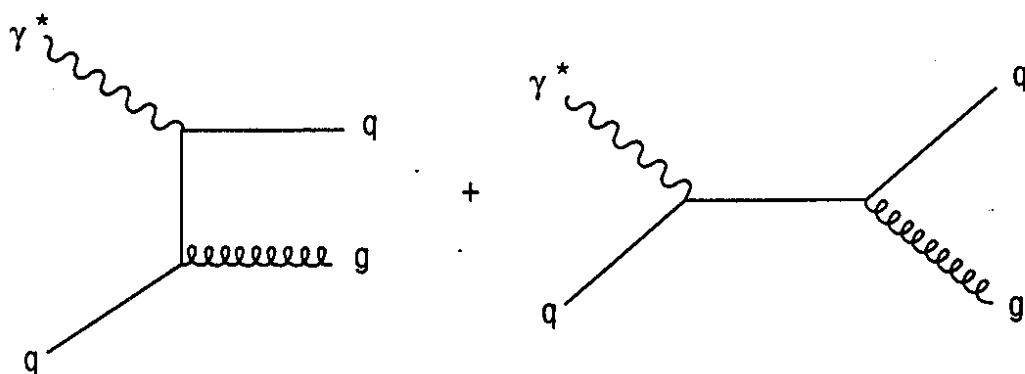**Figure 12:** Feynman diagrams for $\gamma^* q \to gq$.

replaced by a virtual photon. Thus the correction to the vertex may be obtained immediately from Eq. (10.5):

$$i\Gamma^\mu = -ieq_i\gamma^\mu \left[1 + \frac{\alpha_s}{4\pi}\frac{4}{3}\left(\frac{4\pi}{Q^2}\right)^\epsilon \frac{\Gamma(1+\epsilon)\,\Gamma^2(1-\epsilon)}{\Gamma(1-2\epsilon)}\left(-\frac{2}{\epsilon^2} - \frac{3}{\epsilon} - 8\right)\right]. \quad (11.1)$$

The W-boson mass has been replaced by the photon "mass", $q^2 = -Q^2$. Thus the $(-1)^\epsilon$ factor which was present in Eq. (10.5) does not appear in Eq. (11.1).

The real gluon emission corrections to deep inelastic scattering are shown in Fig. 12. The first diagram is infrared divergent, and cancels the infrared divergence (the $1/\epsilon^2$ term) in Eq. (11.1). When we add the virtual and real gluon emission contributions to deep inelastic scattering, we obtain the infrared-finite result for the correction to the quark distribution functions

$$q\left(x, Q^2\right) = q_0\left(x\right)$$

$$+ \frac{\alpha_s}{2\pi}\frac{4}{3}\frac{1}{1-\epsilon}\int_x^1 \frac{dy}{y} q_0\left(y\right)$$

$$\times \left[\left(\frac{1+z^2}{(1-z)_+} + \frac{3}{2}\delta\left(1-z\right)\right)\left(-\frac{1}{\epsilon}\frac{\Gamma(1-\epsilon)}{\Gamma(1-2\epsilon)} + \ln\frac{Q^2}{4\pi}\right)\right.$$

$$+ \left(1+z^2\right)\left(\frac{\ln\left(1-z\right)}{1-z}\right)_+ - \frac{3}{2}\frac{1}{(1-z)_+} - \frac{1+z^2}{1-z}\ln z$$

$$\left. + 3 + 2z - \left(\frac{9}{2} + \frac{\pi^2}{3}\right)\delta\left(1-z\right)\right] \quad (11.2)$$

where $z = x/y$, as always. The $(\quad)_+$ notation is defined in Eq. (10.13).

Differentiating Eq. (11.2) with respect to $\ln Q^2$, we find

$$\frac{d}{d\ln Q^2} q\left(x, Q^2\right) = \frac{\alpha_s}{2\pi}\int_x^1 \frac{dy}{y} q_0\left(y\right) P_{qq}\left(\frac{x}{y}\right) \quad (11.3)$$

where the splitting function

$$P_{qq}(z) = \frac{4}{3}\left[\frac{1+z^2}{(1-z)_+} + \frac{3}{2}\delta(1-z)\right] \tag{11.4}$$

describes a quark coming from quark splitting, $q \to qg$. Eq. (11.3) becomes an Altarelli-Parisi equation, i.e., it sums leading collinear logarithms, when we replace $q_0(y)$ with $q(y, Q^2)$. The full Altarelli-Parisi equation for the quark distribution function, including both $g \to q\bar{q}$ and $q \to qg$, is thus

$$\frac{d}{d\ln Q^2}q(x,Q^2) = \frac{\alpha_s(Q^2)}{2\pi}\int_x^1 \frac{dy}{y}\left[g(y,Q^2)P_{qg}\left(\frac{x}{y}\right) + q(y,Q^2)P_{qq}\left(\frac{x}{y}\right)\right] \tag{11.5}$$

where P_{qg} is given in Eq. (9.2). The running of α_s with Q^2 sums ultraviolet logarithms, as we mentioned in section 9.

12. $p\bar{p} \to W^+ + X$: VIRTUAL AND REAL GLUON EMISSION

We can now combine the corrections to $q\bar{q} \to W^+$ and the quark distribution functions due to virtual and real gluon emission to obtain the $\mathcal{O}(\alpha_s)$ correction to $p\bar{p} \to W^+ + X$. Following steps similar to those in section 8, we obtain

$$\sigma = \sum_{i,j}\int_{\tau_0}^1 dx_1 \int_{\tau_0/x_1}^1 dx_2\left[q_i(x_1,Q^2)\bar{q}_j(x_2,Q^2) + \bar{q}_i(x_1,Q^2)q_j(x_2,Q^2)\right]$$

$$\times \left[\frac{\pi^2}{3}\frac{\alpha}{x_W}\frac{1}{s}\delta(1-\hat{\tau})\right.$$

$$+ \frac{2\pi}{9}\alpha_s\frac{\alpha}{x_W}\frac{1}{s}\left[\frac{3}{(1-\hat{\tau})_+} - 6 - 4\hat{\tau} + 2(1+\hat{\tau}^2)\left(\frac{\ln(1-\hat{\tau})}{1-\hat{\tau}}\right)_+\right.$$

$$\left.\left.+ \left(1+\frac{4}{3}\pi^2\right)\delta(1-\hat{\tau}) + \left(\frac{1+\hat{\tau}^2}{(1-\hat{\tau})_+} + \frac{3}{2}\delta(1-\hat{\tau})\right)2\ln\frac{M_W^2}{Q^2}\right]\right] \tag{12.1}$$

where the first term in the large brackets is the zeroth-order cross section. The collinear divergences of Eqs. (10.14) and (11.2) have cancelled, as expected.

The last term in the $\mathcal{O}(\alpha_s)$ term above, proportional to $\ln M_W^2/Q^2$, can be eliminated via the Altarelli-Parisi equation, Eq. (11.3). Integrating Eq. (11.3) from $\ln Q^2$ to $\ln M_W^2$, we find

$$q(x, M_W^2) = q(x, Q^2) + \frac{\alpha_s}{2\pi}\ln\frac{M_W^2}{Q^2}\int_x^1 \frac{dy}{y}q(y)P_{qq}\left(\frac{x}{y}\right) \tag{12.2}$$

where P_{qq} is given by Eq. (11.4). Using this expression to replace $q(x, Q^2)$ with $q(x, M_W^2)$ in Eq. (12.1), the $\ln M_W^2/Q^2$ term is cancelled, and we are left with

$$\sigma = \sum_{i,j}\int_{\tau_0}^1 dx_1 \int_{\tau_0/x_1}^1 dx_2\left[q_i(x_1,M_W^2)\bar{q}_j(x_2,M_W^2) + \bar{q}_i(x_1,M_W^2)q_j(x_2,M_W^2)\right]$$

$$\times \left[\frac{\pi^2}{3} \frac{\alpha}{x_W} \frac{1}{s} \delta\left(1 - \hat{\tau}\right) \right.$$

$$+ \frac{2\pi}{9} \alpha_s \frac{\alpha}{x_W} \frac{1}{s} \left[\frac{3}{(1-\hat{\tau})_+} - 6 - 4\hat{\tau} + 2\left(1+\hat{\tau}^2\right) \left(\frac{\ln\left(1-\hat{\tau}\right)}{1-\hat{\tau}} \right)_+ \right.$$

$$\left. \left. + \left(1 + \frac{4}{3}\pi^2\right) \delta\left(1 - \hat{\tau}\right) \right] \right] \qquad (12.3)$$

where $s = x_1 x_2 S$, $\hat{\tau} = \tau_0 / x_1 x_2$, and $\tau_0 = M_W^2 / S$. This is our final result for the QCD-corrected cross section for $p\overline{p} \to W^+ + X$ due to virtual and real gluon emission.

We may evaluate the cross section in Eq. (12.3) by using one of the sets of distribution functions mentioned in section 4 and performing the x_1 and x_2 integrations numerically. The relation

$$\int_x^1 dz \left(g\left(z\right)\right)_+ h\left(z\right) = \int_x^1 dz \, g\left(z\right) \left[h\left(z\right) - h\left(1\right)\right] - h\left(1\right) \int_0^x dz \, g\left(z\right) \qquad (12.4)$$

is necessary to perform the integration over the "plus" distributions. The change of variables

$$\hat{\tau} = \frac{\tau_0}{x_1 x_2}$$

$$y = \frac{1}{2} \ln \frac{x_1}{x_2} \qquad (12.5)$$

may be used to obtain $\hat{\tau}$ as an integration variable:

$$\int_{\tau_0}^1 dx_1 \int_{\tau_0/x_1}^1 dx_2 = \int_{\ln\sqrt{\tau_0}}^{-\ln\sqrt{\tau_0}} dy \int_{\tau_0}^1 d\hat{\tau} \, \frac{\tau_0}{\hat{\tau}^2}. \qquad (12.6)$$

Performing the required integrations, we find that the $\mathcal{O}\left(\alpha_s\right)$ correction to $p\overline{p} \to W^+ + X$ from virtual gluons and gluon radiation at $\sqrt{S} = 1.8$ TeV is about 33% of the zeroth-order cross section, and positive. Adding this to the negative 7% correction from initial gluons, we find that the $\mathcal{O}\left(\alpha_s\right)$ corrections to $p\overline{p} \to W^+ + X$ at the Tevatron increase the zeroth-order cross section by about 26%. The corresponding increase at the CERN collider ($\sqrt{S} = 630$ GeV) is about 30%. The systematic error in the measured cross section is about 10%, and the statistical error is much less, since over one thousand events have been observed. The QCD correction to $p\overline{p} \to W^+ + X$ is therefore observable, in principle. Uncertainties in the parton distribution functions introduce some ambiguity in the calculated cross section, but hopefully these uncertainties will be reduced to a level where we can unambiguously observe the QCD correction to $p\overline{p} \to W^+ + X$.

Numerically, the most important term in the $\mathcal{O}\left(\alpha_s\right)$ correction to $p\overline{p} \to W^+ + X$ is the π^2 term in Eq. (12.3). Since this term is proportional to $\delta\left(1-\hat{\tau}\right)$, it arises from the kinematic region $s = M_W^2$, which corresponds to a virtual gluon or

soft gluon radiation. This π^2 term arose in the loop correction to $q\bar{q} \rightarrow W^+$ from expanding $(-1)^\epsilon$ (Eq. (10.6)) and $\Gamma(1 + \epsilon)\Gamma(1 - \epsilon)$ (Eq. (10.8)) to $\mathcal{O}(\epsilon^2)$, and multiplying by the $1/\epsilon^2$ term in Eq. (10.5). Since the $1/\epsilon^2$ term corresponds to an infrared divergence, we see that the π^2 term is related to the infrared region. The QCD correction to the quark distribution function also contains a π^2 term, from expanding $\Gamma(1 + \epsilon)\Gamma(1 - \epsilon)$ in the loop correction to $\gamma^* q \rightarrow q$. Since there is no factor of $(-1)^\epsilon$ in this loop correction, the π^2 term differs from that of $q\bar{q} \rightarrow W^+$.

Since the π^2 term is proportional to $\delta(1 - \hat{\tau})$, it is proportional to the zeroth-order cross section. Thus the π^2 term corrects the total cross section by a multiplicative factor

$$K = 1 + \frac{\alpha_s}{2\pi}\frac{4}{3}\frac{4}{3}\pi^2 \tag{12.7}$$

which is often called the "K factor." One factor of $4/3$ in Eq. (12.7) is from color $(T^A T^A = \frac{4}{3}\mathbf{1})$ and the other is from summing the various contributions to the π^2 term outlined above.

Originally, the entire $\mathcal{O}(\alpha_s)$ correction to the Drell-Yan process was called the K factor, although this is a misnomer since the correction is not an overall factor. This correction is often approximated by the numerically dominant π^2 term, via Eq. (12.7), which has now come to be called the K factor. Of course, Eq. (12.7) is only an approximation to the full $\mathcal{O}(\alpha_s)$ correction to $p\bar{p} \rightarrow W^+ + X$, given by Eqs. (9.5) and (12.3).

ACKNOWLEDGEMENTS:

REFERENCES

1. For a review of the early experiments, see J. Friedman and H. Kendall, Ann. Rev. Nucl. Sci. <u>22</u>, 203 (1972).

2. Reminiscences of Feynman and the parton model can be found in J. Bjorken, Physics Today <u>42</u>, February 1989, 57 (1989).

3. W. Marciano and H. Pagels, *Quantum Chromodynamics*, Phys. Rept. <u>36C</u>, 137 (1978).

4. G. Altarelli, *Partons in Quantum Chromodynamics*, Phys. Rept. <u>81</u>, 1 (1982).

5. J. Kubar-André and F. Paige, Phys. Rev. <u>D19</u>, 221 (1979).

6. G. Altarelli, R.K. Ellis, and G. Martinelli, Nucl. Phys. <u>B157</u>, 461 (1979).

7. M. Glück, E. Hoffmann, and E. Reya, Z. Phys. <u>C13</u>, 119 (1982).

8. D. Duke and J. Owens, Phys. Rev. <u>D30</u>, 49 (1984).

9. E. Eichten, I. Hinchliffe, K. Lane, and C. Quigg, Rev. Mod. Phys. <u>56</u>, 579 (1984).

10. A. Martin, R. Roberts, and W. Stirling, Phys. Rev. <u>D37</u>, 1161 (1988); Phys. Lett. <u>206B</u>, 327 (1988).

11. M. Diemoz, F. Ferroni, E. Longo, and G. Martinelli, Z. Phys. <u>C39</u>, 21 (1988).

12. W.-K. Tung, in *Physics Simulations at High Energy*, eds. V. Barger, T. Gottschalk, and F. Halzen (World Scientific, Singapore, 1987), p. 601; J. Collins and W.-K. Tung, Nucl. Phys. <u>B278</u>, 934 (1986).

13. J. Collins, D. Soper, and G. Sterman, Nucl. Phys. <u>B308</u>, 833 (1988).